Stockholm University

Master Thesis

Degree Project in Geochemistry 45 hp

Spatial and temporal variability of the water isotopes in the snow-pack across central Sweden: links to the NAO

Barkas Charalampos

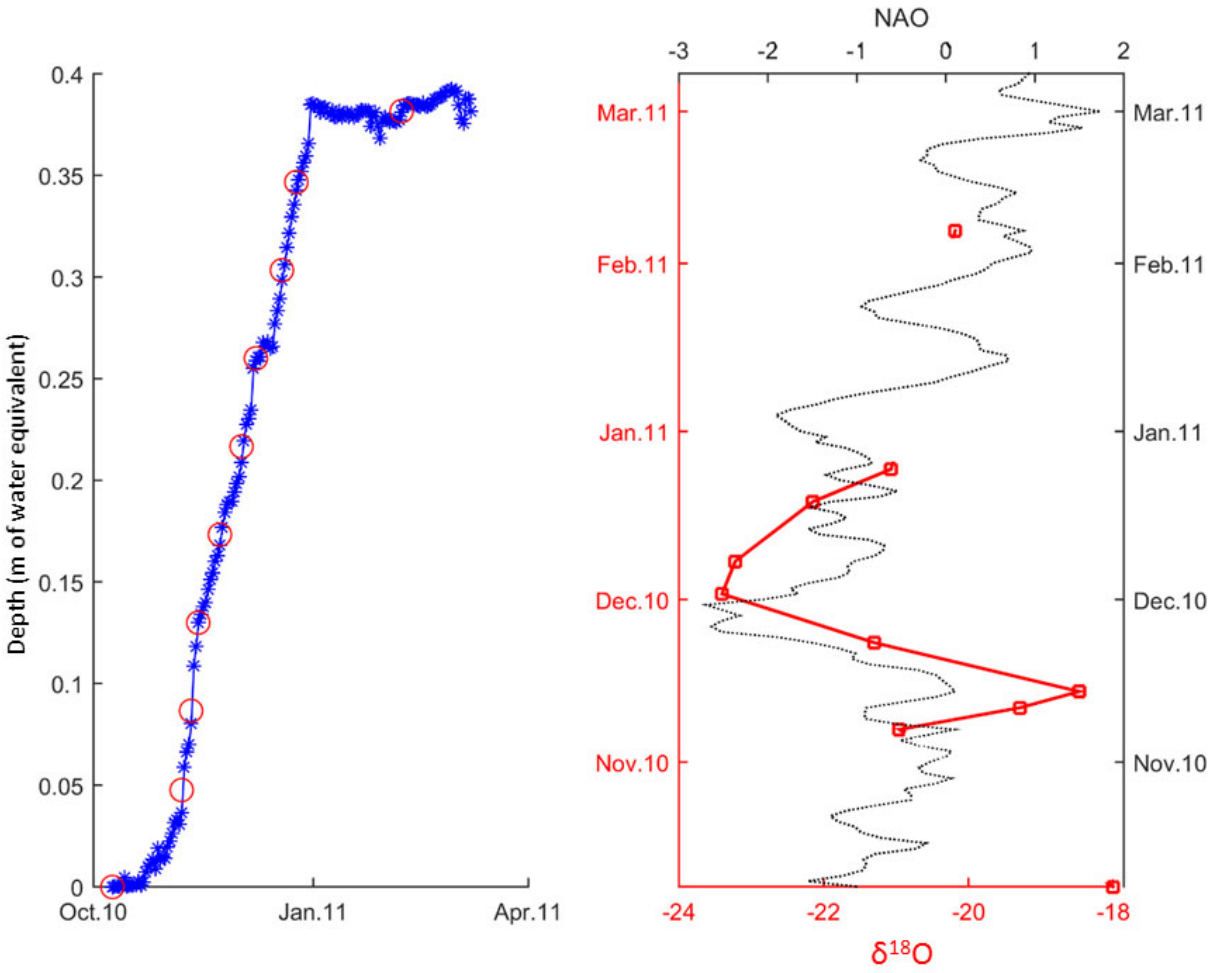

Stockholm 2016

Department of Geological Sciences
Stockholm University
SE-106 91 Stockholm

Contents

Abstract 2
1 Introduction 3
1.1 The North Atlantic Oscillation (NAO) 3
1.2 Stable Water Isotopes (SWI) 5
1.3 Study area and study region 7
2 Material – Method 8
2.1 Sampling - Field measurements - In situ data 8
2.2 Data 10
2.3 Age-depth Model/Algorithm 10
3 Results 12
3.1 Age-depth Model/Algorithm 12
3.2 Correlation NAO - $\delta^{18}O$ in central Sweden (study region) 14
4 Discussion 18
4.1 Age-depth Model/Algorithm 18
4.2 Correlation NAO - $\delta^{18}O$ in central Sweden (study region) 20
4.3 Thoughts (Thesis Considerations) and future prospects 22
5 Conclusions 23
References 24
Appendix 30

Abstract

The objective of this master thesis is to investigate the spatial and temporal variability of the Stable Water Isotopes (SWI) in the snow-pack across central Sweden and how these are related on the North Atlantic Oscillation (NAO). The North Atlantic Oscillation has changed in the last 30 years and these changes affect the climate in the North hemisphere. In order to clarify its effects, it is important to understand the NAO variations and how its signature is characterized spatially and temporally. Isotopic composition in precipitation is a key parameter related to atmospheric phenomena. Stable water isotopes in each snow-core have been used in order to detect temporal variation in isotopic composition in annual precipitation. For the aim of this thesis, 2415 snow samples which correspond to 143 snow-cores, sampled from 2010 to 2015. A new age-depth algorithm have been established in order to connect each snow-depth with a certain date automatically. Snow depth from ERA Interim dataset have been inserted to the model in order to calibrate/adjust the field measurements. Estimations of the correlation coefficient (R) between the daily NAO index and the $\delta^{18}O$, reveal a typical pattern. More specifically, central Scandinavia is divided in three zones with similar characteristics. The First (northern) zone and the third (southern) zone represent areas with positive correlation coefficient 'R' (NAO - $\delta^{18}O$) while the zone 2 depicts a negative correlation coefficient 'R' (NAO - $\delta^{18}O$).

Keywords: Snow-cores, Stable water isotopes (SWI), North Atlantic Oscillation (NAO), Age-depth model/algorithm, central Scandinavia

1 Introduction

Many studies have shown a relationship between atmospheric circulation and isotopic composition in precipitation(Serreze et al. 2000; Dergachev and Vasiliev 2004; Welker, Rayback, and Henry 2005; Insel et al. 2013). In addition, stable water isotopes from ice cores help to achieve an understanding of climate signals in various areas in the earth (Aizen et al. 2005; Tian et al. 2006). Those two statements guide us to start working on this study.

This study focuses on spatial and temporal variability of the stable water isotopes (SWI) in the snow pack, and its correlation to North Atlantic Oscillation (NAO). This project has extended over 6 years (2010-2015) and attempts to investigate the annual effect of NAO in central Sweden's climate. In addition to snow samples from 2015 collected during the present study, observations/data from the previous years (2010-2014) used for analysis. The total amount of snow samples are 2415 and cover spatially almost the central/northern Sweden and the central Norway. That approach has an advantage that allows to collect records of all winter's precipitation in a single core sampling. However, ice/snow-cores can indicate a climate signal only if precipitation occurs (Werner et al. 2000) and as a result at the same advantage also becomes a limitation.

One central objective of this project is to retrieve meaningful information for improving future campaigns and reaching accurate results, such as appropriate sampling locations, clarify/specify uncertainties and general to be a base for future analysis.

1.1 The North Atlantic Oscillation (NAO)

The North Atlantic Oscillation (NAO) is an atmospheric phenomenon in the North Atlantic Ocean defined as the sea-level pressure difference between the Subpolar Low (Iceland) and the Subtropical High (Azores) (Thompson, Lee, and Baldwin 2003). It alternates between two phases, negative and positive. This phenomenon is one of the oldest known global weather patterns, descriptions occurred from nautical Scandinavians a few centuries ago (Mills 2004). Because of the NAO structure (interaction between atmospheric storms), it is difficult and crucial to predict the width, magnitude and phase of it (Hurrell et al. 2003a). Also, this variability in the form of the NAO derives from internal atmospheric processes (Visbeck et al. 2001). However, there is a renewed interesting about NAO, recently (Hurrell et al. 2003a). The interpretation is, that NAO has changed in the last 30 years (Thompson and Wallace 1998; Thompson and Wallace 2000; Welker, Rayback, and Henry 2005). A noteworthy characteristic of the NAO is its trend toward a more positive phase over these 30 years (Hurrell 1995). Additionally, NAO effects are strongest the 20th centuries and weaker in the previous years (Jones, Osborn, and Briffa 2003) (fig.1).

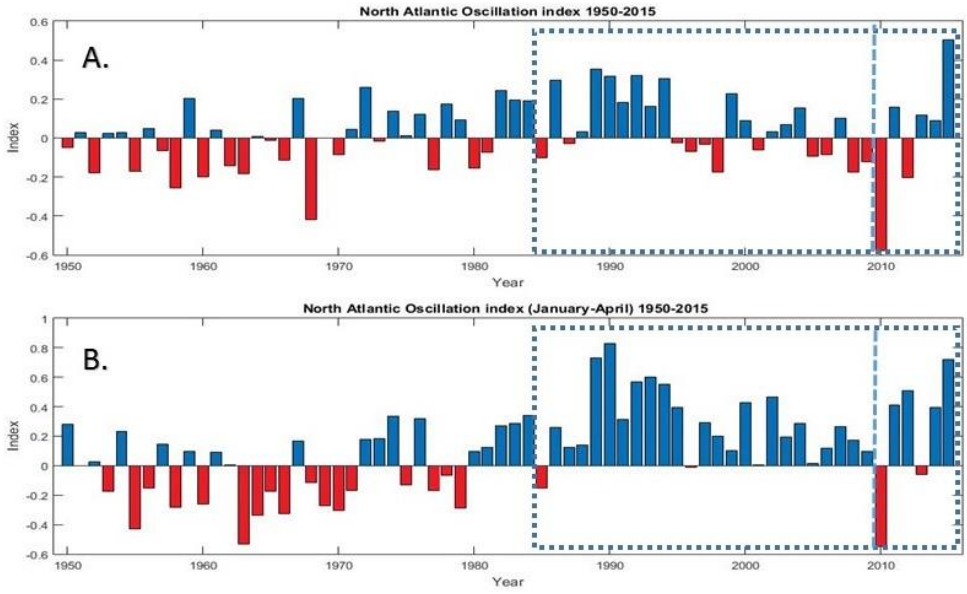

Figure 1: North Atlantic Oscillation. A. Mean annual index B. Mean snow period (January – April) index. 30 last years and the campaign years are indicated by blue dashed lines. Results based on daily NAO index (source: http://www.cpc.ncep.noaa.gov/).

This graph in fig.1 illustrates the abovementioned trend that positive phase prevails the last 30 years. Numerically, the average annual index from 1950 to 1984 is -0.006 and from 1985 to 2015 is 0.05. Counting only the snow period (Jan-April), the growth becomes more evident for the same periods from 0.028 (1950-1984) to 0.27 (1985-2015), respectively.

NAO's fluctuations influence temperature, precipitation, and atmospheric circulation over the north hemisphere (Hurrell and Loon 1997; Cook 2003) , and NAO is considered as the dominant phenomenon of European climate variability. The magnitude of correlation between surface climate and NAO differ with time, according certain studies (Osborn et al. 1999; Jones, Osborn, and Briffa 2003). The NAO pattern is associated with increased water temperatures in one part of the Atlantic ocean and cold them in another (Hurrell et al. 2003a). Small scale effects of NAO are the amount as well as the strength of storms. By taking the above mentioned into consideration it can be said that the NAO has a constant impact on the physics, hydrology, chemistry and biology of freshwater ecosystems (Straile et al. 2003). Finally, it influences all the humans' infrastructure, in particular hydropower. A certain example, in the study area, is the following; significant fluctuations in temperature and precipitation because of NAO over Scandinavia between 1995 and 1996 guide studies to exam the availability of water in Scandinavia for hydropower generation (Seager et al. 2000).

Impacts become larger from mid to high latitudes climate, influencing precipitation or/and temperature on daily and annual bases (Wanner et al. 2001; Hurrell et al. 2003b). The recent positive trend in the NAO increases the temperature specially in Europe and Asia (Hurrell 1996). In winter, the NAO's perturbations having the largest amplitude and occur strong influences on winter's temperature and precipitation (Hurrell et al. 2003a).

Positive phase of the winter NAO has led to raise the frequency and power of storms (Hurrell and Loon 1997) from 1980s and Sweden's climate has become more mild and wet (Visbeck et al. 2001; Lindström and Alexandersson 2004). During negative winter NAO phases, Scandinavia is dominated by cold and dry conditions (St. Amour et al. 2010). A positive summer NAO phase produces warm and dry conditions over northwest Europe and Scandinavia (Folland et al. 2009).

1.2 Stable Water Isotopes (SWI)

Climate phenomena such as the NAO and Southern Oscillation Index (SOI) have a significant impact of spatial and temporal variation in isotopic composition in precipitation all over the world (Liu et al. 2014). More particularly, in Scandinavia and general in the northern hemisphere changes in isotopic composition of precipitation has been attributed to the North Atlantic Oscillation (Baldini et al. 2008). This impact is not only annual but can have seasonal patterns of precipitation and transform water (oxygen and hydrogen) isotopes composition (Bowen and Wilkinson 2002).

The isotopic composition (the proportion of $H_2{}^{18}O$ and HDO) in the water samples can be measured using mass or laser spectrometer. The definition of them is described in the following equations.

$$\delta^{18}\text{O} = \left(\frac{R1_{sample}}{R1_{V-SMOW}} - 1 \right) \times 10^3 \quad \text{(Equation: 1)}$$

$$\delta D = \left(\frac{R2_{sample}}{R2_{V-SMOW}} - 1 \right) \times 10^3 \quad \text{(Equation: 2)}$$

Where, $R1 = \frac{[H_2^{18}O]}{[H_2^{16}O]}$, $R2 = \frac{[HD^{16}O]}{[H_2^{16}O]}$ and V-SMOW stands for the Standard Mean Ocean Water. The World Meteorological Organization (WMO) and the International Atomic Energy Agency (IAEA) begun the Global Network for Isotopes in Precipitation (GNIP) in 1961 (Schotterer, Oldfield, and Froehlich 1996).

A key factor in understanding the global water cycle is the geospatial distribution of the water isotopes (Rozanski, Araguás-Araguás, and Gonfiantini 1993); in relation with several meteorological parameters. Stable water isotopologues ($H_2{}^{18}O$ and HDO), usually referred to as stable water isotopes (SWI) (Sturm, Zhang, and Noone 2010), offer a great potential for investigating atmospheric circulation (Aggarwal et al. 2004) or land surface (i.e., elevation, vegetation) parameters (Insel et al. 2013). Many of hydrological, hydrogeological and hydroclimate investigations relied on the exploitation of SWI (Darling 2004; Labuhn et al. 2015) (fig. 2).

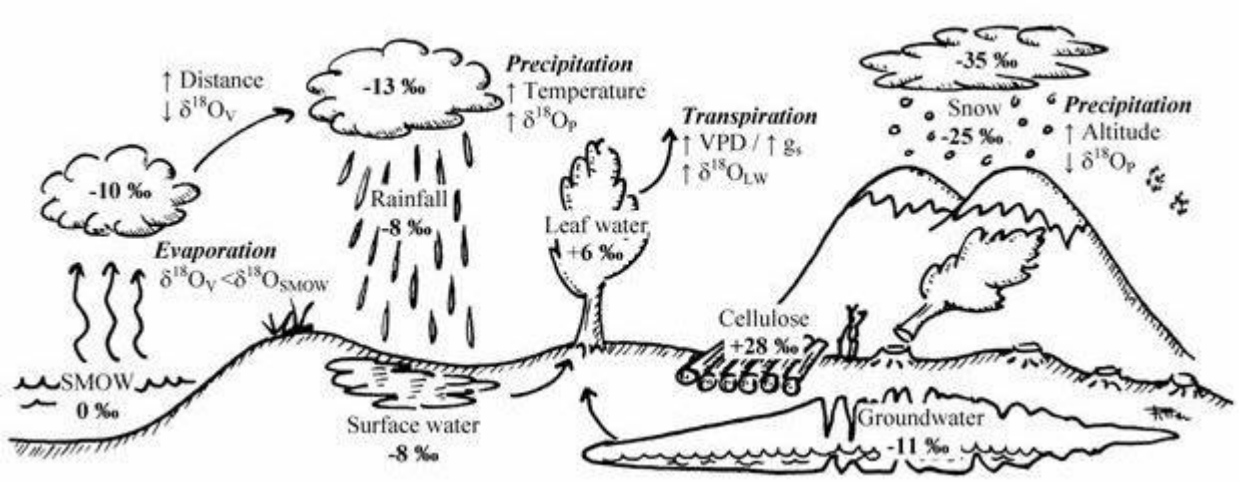

Figure 2: Main fractionation steps and typical values of oxygen isotope composition ($\delta^{18}O$) in a temperate climate (source: http://web.udl.es/).

Water isotopic composition depends on the isotopic composition of their source water, which is later altered by processes along its trajectory; evaporation, biochemical reactions and kinetic fractionation (Labuhn et al. 2015). Changes in the seasonality of precipitation (temporal variations) can also affect the average annual precipitation $\delta^{18}O$ (Harris et al. 2014).

Useful information regarding moisture source and precipitation's history and/or seasonality can be derived from SWI utilization (Charles et al. 1994; Hammarlund et al. 2002; Jouzel 2003). Many studies use SWI for paleoclimate reconstruction (Petit et al. 1999; McDermott 2004; Kress et al. 2010). Ice core studies (sampling polar caps and glaciers) aiming to determine temperature index have used $\delta^{18}O$ and δD as key components (Thompson et al. 2003; Fujita and Abe 2006).

Other studies in Greenland have examined the correlation or not between the NAO and $\delta^{18}O$ in ice/snow cores (White et al. 1997; Vinther et al. 2006). Apart from this, model studies (Sjolte et al. 2011) have probed the influence of the NAO on Greenland's water isotope composition.

Finally, a second-order parameter, the deuterium excess (d_excess) is calculated as

$$d\_excess = \delta D - 8 \times \delta^{18}O \quad \text{(Equation: 3)}$$

The deuterium excess can maintain information about kinetic fractionation taking place during evaporation at the ocean and during snow formation (Merlivat and Jouzel 1979; Steen-Larsen et al. 2011). Examining sea surface temperature the deuterium excess is a useful indicator (Fujita and Abe 2006).

1.3 Study area and study region

The study area covers several sites across Scandinavia (fig.3). Scandinavia is located in north-west part of Europe (N:70° S:55° W:5° E: 23°). Atlantic Ocean and Baltic Sea are the sea boundaries from west to east. The Scandes is a mountain range between Norway and Sweden that influences the amount of annual precipitation in those countries. In general terms, the climate across central Scandinavia, from west to east, transitions to oceanic–continental–oceanic (Busuioc, Chen, and Hellström 2001). Because of the Gulf Stream, Sweden has mild climate comparing with other countries in the same latitude (ex. Canada). February is the coldest month and the mean temperature varies from -3 °C to -22 °C. The mean annual precipitation differ from 500 mm to 800 mm according to locations.

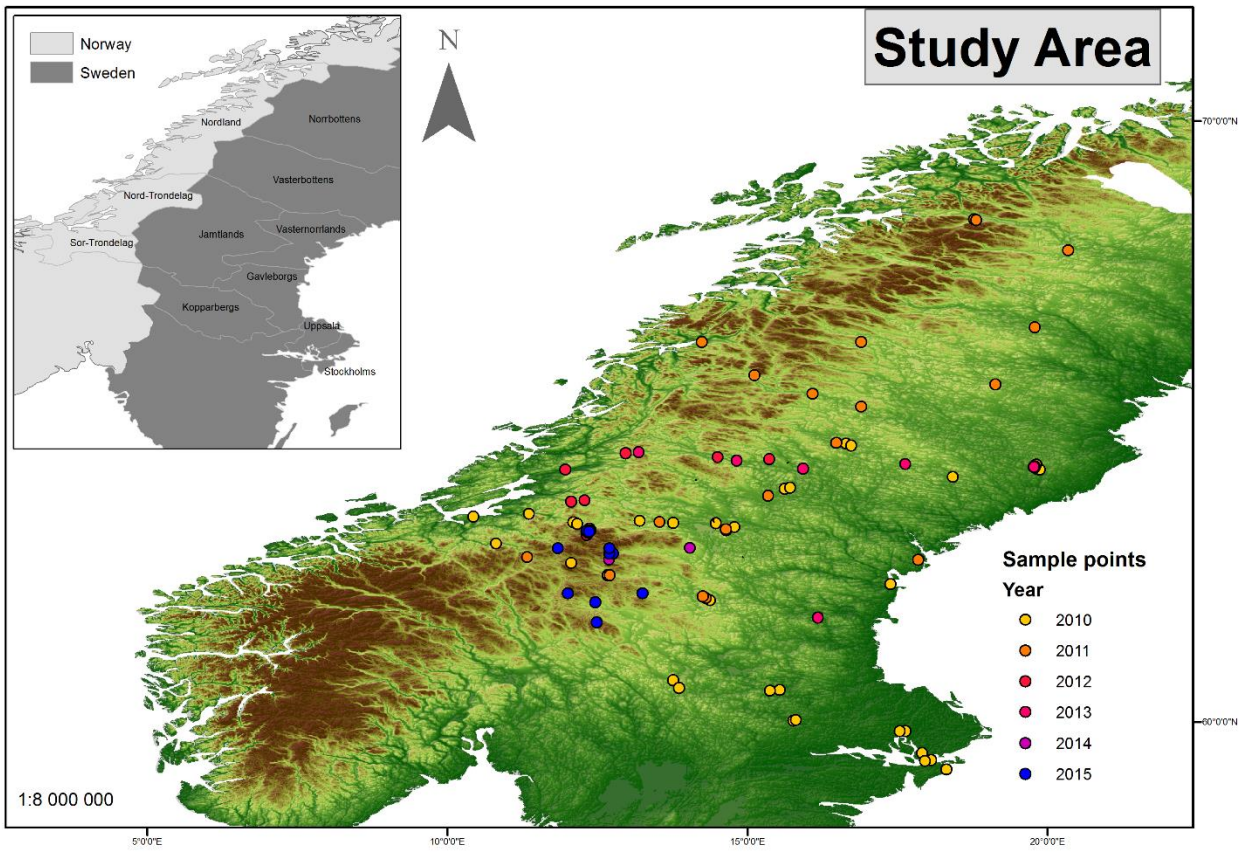

Figure 3: Study area. Sampling site from different years are presented in different colors.

Scandinavian climate is also effected by the North Atlantic, and its westerly gale bringing heat and moisture. Those winds change altitude on the Scandinavian Mountains (Scandes). The Scandes is a topographic threshold that divides Scandinavia in discrete zones (east-west and north-south) according to the temperature and moisture (St. Amour et al. 2010). However, the balance between Arctic and North Atlantic air masses rules the atmospheric circulation in Scandinavia (Hurrell et al. 2003a; Rosqvist et al. 2013).

2 Material – Method

2.1 Sampling - Field measurements - In situ data

The present study includes snow samples from winter seasons 2010 to 2015. For this thesis in situ data collected during 2015 (11th- 16th of April) over central Sweden and Norway. 10 snow-cores and fresh snow have been collected and provided us with 196 unique snow/water samples for 2015. The measurements made on two level included GPS position and snow depth.

Sample sites for the 2015 campaign were chosen based on the geographical location of the previous years in order to enhance the outcome or/and to clarify some uncertainties of earlier years. The sampling areas are snow–free during summer and as result each snow-core contains one winter snow.

The protocol for previous campaign included only the Russian corer (fig.4) to be the sample tool, many cores in 2015 are collected in a snow pit (digging with shovel) (fig.5), for practical reasons at remote

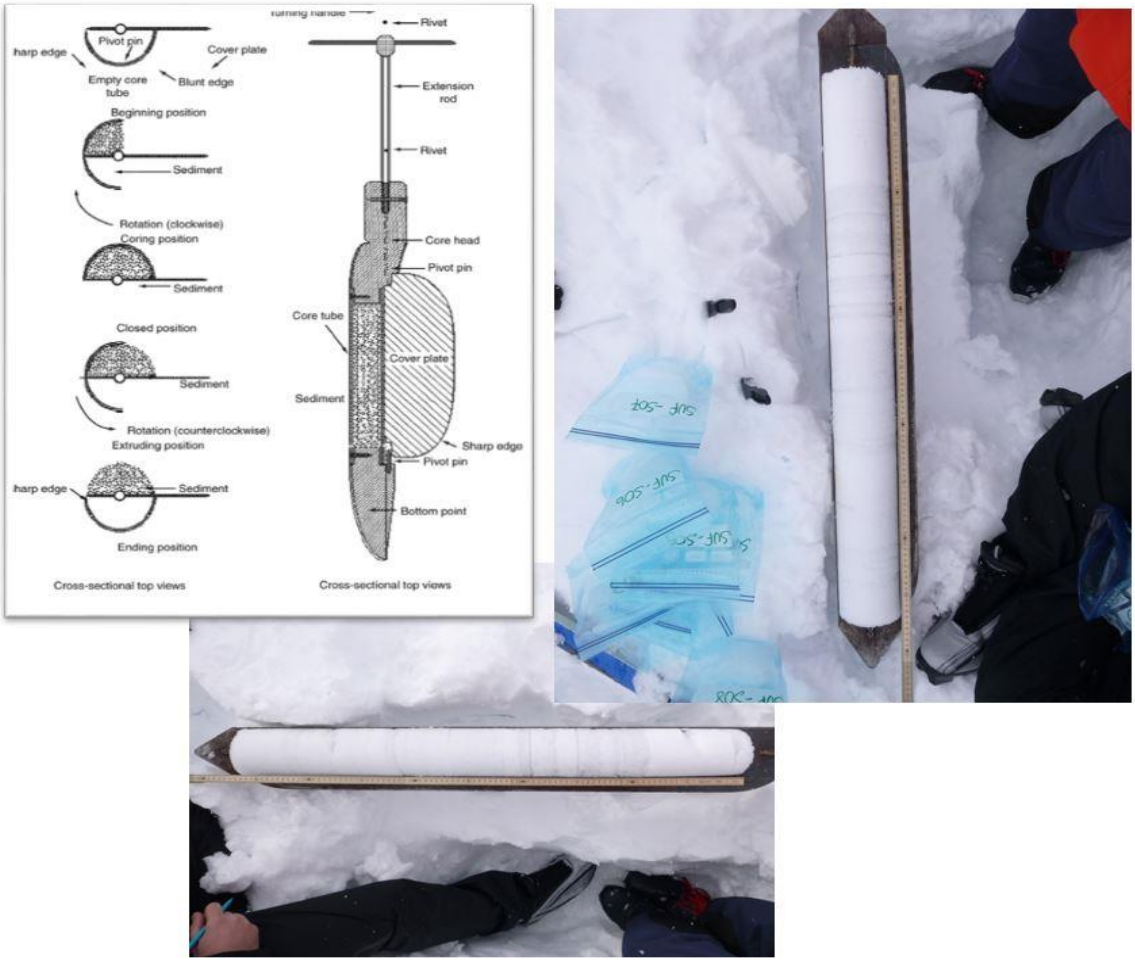

Figure 4: Russian corer. Sampling according to the protocol. (Left picture's source: https://clu-in.org/programs/21m2/sediment/), field work pictures (right and bottom).

sampling sites. One reason for adopting the protocol is that the Russian corer has length only one meter where in many sites the snow depth was much higher. Another major reason is that the Russian corer is very heavy (20 kilos) and it is complicated to carry it for long distances (many kilometers). Sampling in a snow pit has also drawbacks, it is more time consuming and the volume of the individual slice samples are not always well constructed; hence density can no longer be estimated. After, each snow core was divided consecutively into 5 cm slices starting from the surface. Finally, the samples were stored in plastic airtight bags in order to avoid any leakage which could alter the sample's isotopic composition.

Figure 5: Sampling in a snow pit (field work pictures).

2.2 Data

Water isotope analyses of snow samples were performed in Stable Isotope Laboratory (SIL) at the Stockholm University under the supervision of Heike Siegmund. Samples are analyzed with a Picarro L2140-i wavelength-scanned cavity ring-down spectroscopy (WS-CRDS) by exploiting the principles of laser absorption method. According to its manual the analysis precision is 0.025 ‰ for $\delta^{18}O$ and 0.1 ‰ for δD (fig.6).

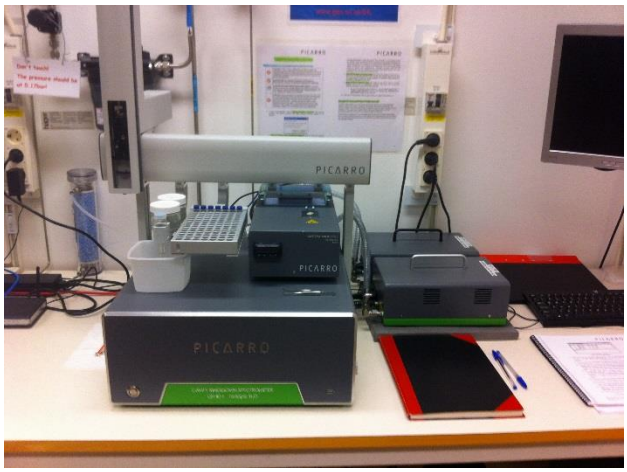

Figure 6: Picarro L2140-I in stable isotope laboratory at SU.

We used ERA Interim dataset ECMWF (Dee et al. 2011) for estimates of following variables : snow depth (sd : [m of water equivalent]), total precipitation (tp : [m]) and snow density (rsn: [kg * m^{-3}]). We chose the study period from September 1999 to May 2015. The temporal resolution is 24 hours (daily) and the spatial 0.125° by 0.125° (~ 15 by 15 km).

U.S. National Weather Service provided, for this study, with the daily NAO index since January 1950. For the first 50 years (1950 – 2000) daily value has been standardized by standard deviation of the monthly NAO index interpolated to day (http://www.cpc.ncep.noaa.gov/).

Digital Elevation Model (DEM) from USGS EROS Data Center with a grid spacing 30 arc seconds (1 km) over for the Scandinavia used. All the datasets were in geographic coordinates system (GCS_WGS_1984).

2.3 Age-depth Model/Algorithm

In order to establish an automated age-depth profile for each sample site and year all data inserted in MATLAB R2015a. Each location has a unique structure, including the date of sampling, coordinates and SWI results ($\delta^{18}O$ and δD), as illustrated in Appendix table 1.

Identifying the true location of each site in the grid, nearest neighbor interpolation was used. For each site and year the first day of snow is described as the next day after the first day without snow from the

date of sampling and backwards (the first snow slice closes to ground corresponds to that day). The last day is the sampling day. The outcome of this process, is to have a daily snow depth profile for each core.

Difference between local observed snow depth and ERA 15×15km menu grid value Interim dataset snow depth, were scaled with a 'unique coefficient'. It is introduced in order to match the observed snow depth with ERA Interim dataset (sd). This 'scaling coefficient', unique to each sampling site, is estimated dividing the snow depth value from ERA Interim dataset with the observed snow depth in sampling date.

To attribute a date to each snow slice's SWI analysis, we make the assumption that the considered day not only should have the same snow depth value as the ERA Interim dataset but also must be the last day of the whole period (with this snow depth) when the snow depth is increasing (more than one day might have the same snow depth value in the considered winter due to snow melt processing).

First approach to define the correlation is the 'qualitative comparison'. Printing the outcome of the daily $\delta^{18}O$ and deuterium excess (d_excess) records and comparing them visually with daily NAO index schematically. This comparison allows the studier to overlap some uncertainties such as neglecting extreme values. 'Qualitative comparison' help us to understand the outcome, visualize the result and continue the study with 'quantitative correlation'.

The 'quantitative correlation' between NAO - $\delta^{18}O$ and NAO - deuterium excess (d_excess) calculated based on the daily NAO index and the estimated-daily records of $\delta^{18}O$ and δD. (Appendix, table 2 presents the model/algorithm).

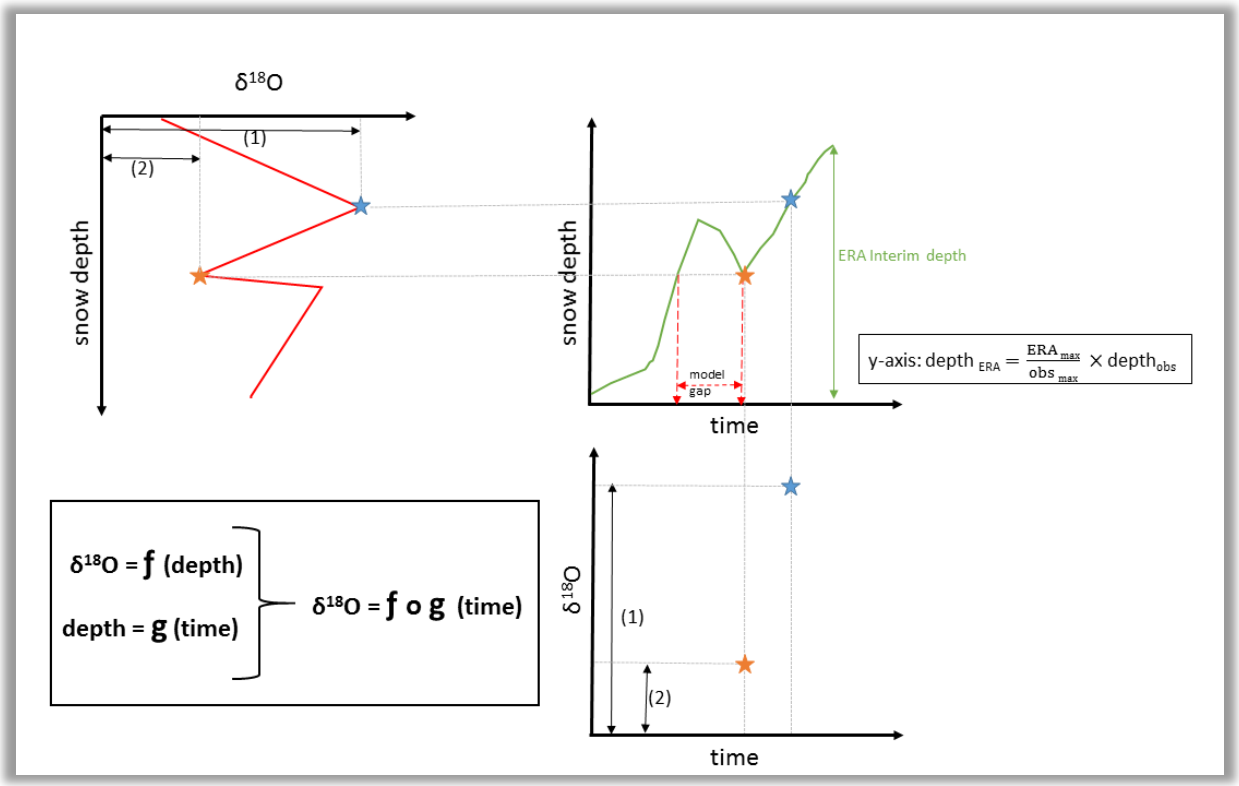

Figure 7: Conceptual model. Basic idea for Age-depth model (inserted data and final result).

3 Results

3.1 Age-depth Model/Algorithm

The Matlab script estimates the age-depth profile for each sample site. The performance of model was evaluated by plotting each sample core against date (fig.8). This approach can lead to more meaningful assessment and interpretations and improve the detectability of potential uncertainties. In general, figure 8 illustrates the estimated dates for each slice of snow. Algorithm sets the 'first day' of snowfall based on methods (the next day after the first day without snow reading from the date of sampling and backwards). However, the 'last day' does not always coincide with the sampling day; this is because the age-depth

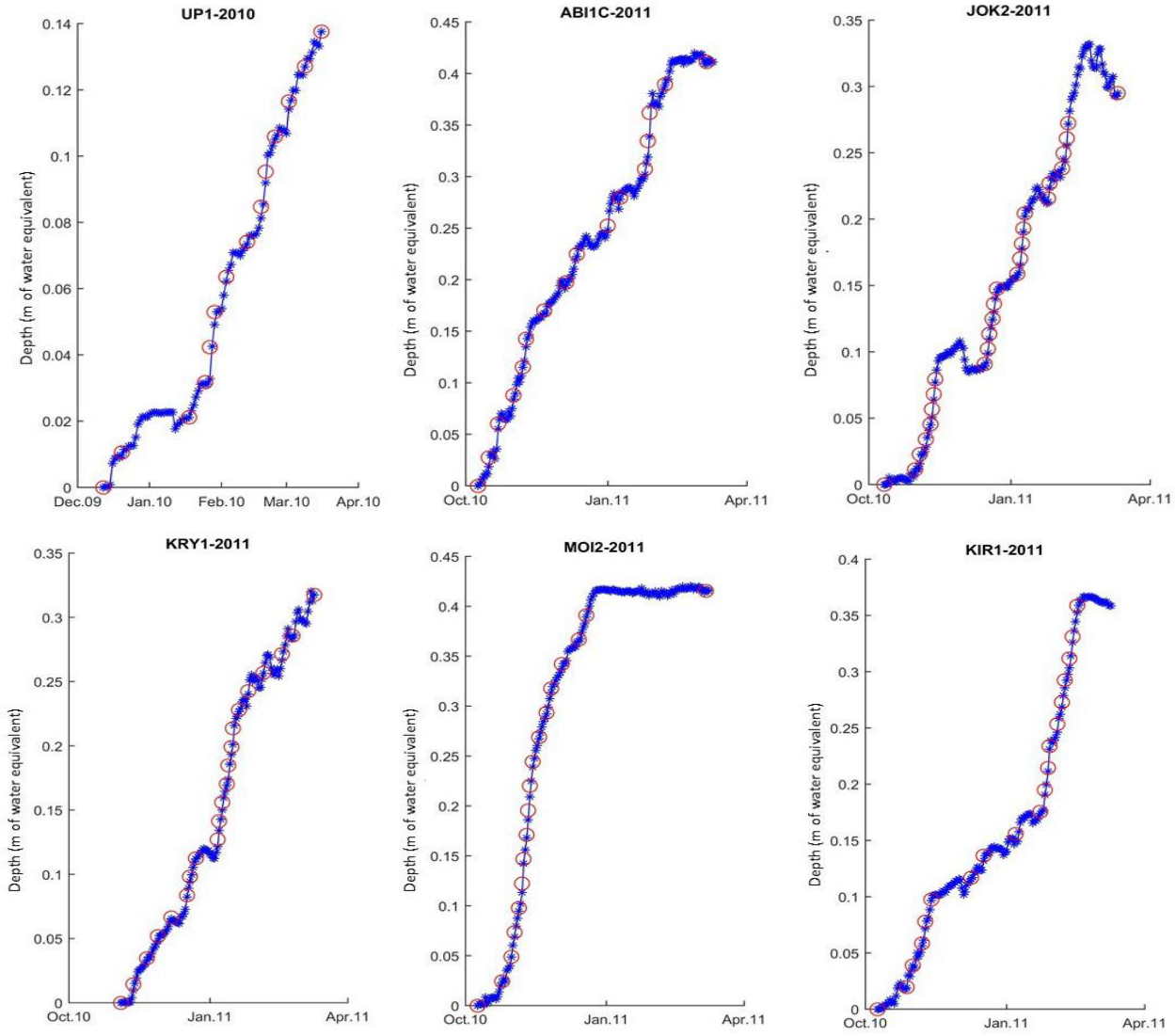

Figure 8: Visualization of age-depth profiles. Title is the site name - year of sampling. Blue line is the snow depth according to ECMWF (m of water equivalent). Blue line starts the first day of snow based on methods and ends the sampling date. Blue stars are different days. Red cycles shows the corresponding date and depth for each ice slide.

model detects the precipitation (snowfall) event. Despite of that the algorithm approach provides us with reliable results, as discussed in the next chapter.

Secondly, using this depth-date transfer function, the isotopic composition of each snow sample has been plotted versus time alongside daily NAO. These plots enable to visualize the uncertainties of the model for 'correlated' or 'anti-correlated' sites to the NAO; specially, when the proposed model is new and further improvements may be needed. Although, 'the qualitative approach' has not been included to the analysis of the correlation, it is useful to be presented (fig. 9).

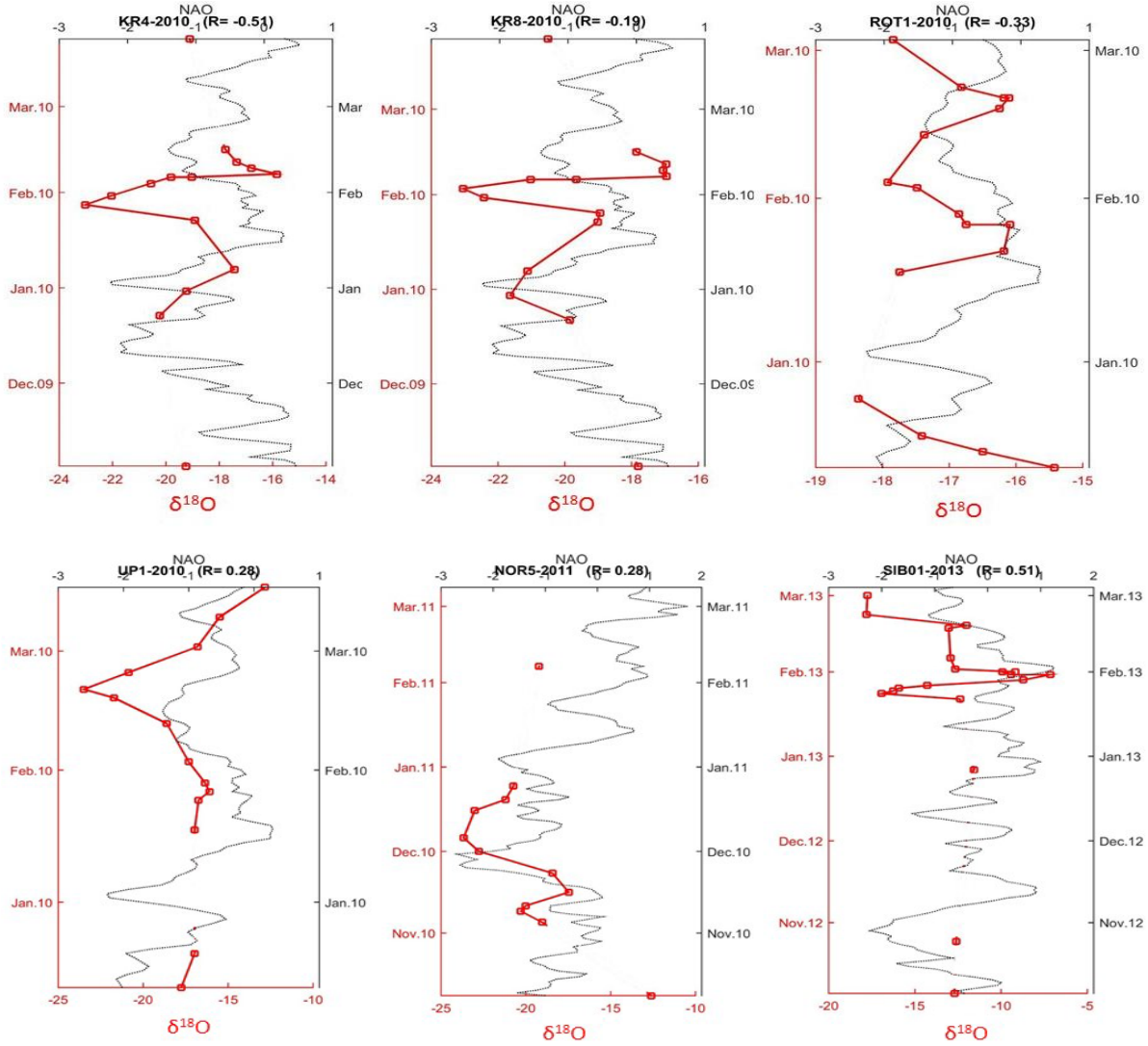

Figure 9: Examples of plots $\delta^{18}O$ and daily NAO against date. Title is site name – year and correlation coefficient R ('qualitative approach') between $\delta^{18}O$ and the daily NAO index. Red line is the daily isotopic composition ($\delta^{18}O$) and black line is the daily NAO index.

Observing the figures, it is sometimes ambiguous whether shifting the dates (red line) forwards/backwards, within the dating uncertainties, the result of the correlation coefficient (R) may be

better or completely different. *KR8-2010* can be characterized as a 'no correlated' place (R=-0.19) but it seems that the pattern of the red line tends to mirror the daily NAO (black line). Another noteworthy example is the *KR4-2010*. In that location the arithmetical result of the correlation coefficient equals -0.51 but it can be optimized by shifting the dates (points) on the first days of February.

Even if, a number is not always indicative of real conditions, for the purposes of this research only the 'quantitative approach' was taken into consideration. 'Qualitative approach' performed at first, to assess the validity of NAO - $\delta^{18}O$ similarity. 'Qualitative approach' aimed to validate the age-depth model and then 'quantitative approach' applied to present/express the result. Another motivation that supports the exploitation of 'quantitative approach' is the fact that statistics cannot be easily refuted.

The locations were subdivided into 5 categories (fig.10). According to the correlation coefficient between NAO and $\delta^{18}O$, the categories are *nn, n, m, y* and *yy*. Negative correlation (anti-correlated locations) is depicted with *n* and red color while positive correlation represented by *y* symbol and blue color. Sample sites with correlation coefficient (R) values between -0.2 and 0.2 are characterized as 'no correlated'. Consequently, these sites were excluded from the analysis (in appendix. Table 1 lists in detail all the sampling sites and their results).

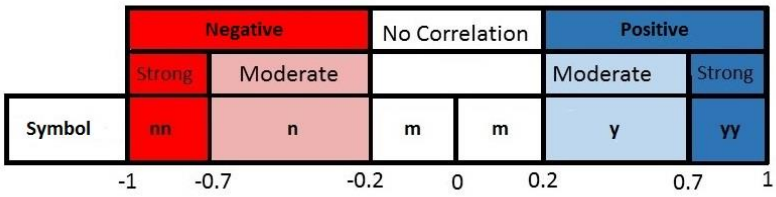

Figure 10: Correlation Coefficient 'R' scale. Negative correlated is a location when its R is from -1 to -0.2. Positive correlated is a location when its R is from 0.2 to 1. Dark and light color provides information about the strength of the correlation.

3.2 Correlation NAO - $\delta^{18}O$ in central Sweden (study region)

Once the 'quantitative approach' was performed, the outcome for each location was imported to ArcMap 10.2.2. for further analysis. The map (fig.11) visualizes the numerical correlation coefficient derived from the algorithm and presents the spatial correlation of the isotopic composition of each area and the NAO. As it can be seen, the spatial distribution of the snow-cores is not homogenous over Scandinavia. Hence, we chose the suitable domain, a sub-area of Scandinavia (study region). Key components for the suitability of this selection were the number of samples per square kilometer and the elevation. Furthermore, the study region is the only area where sampling was carried out during every campaign (2010-2015). Low altitudes areas are also more affected by post deposition effects (e.g., melting).

The selected study region is situated in the central Scandinavia in and around Jämtland (fig.12) and is characterized by high altitude. Its total extent is approximately equal to 100,000 km^2. During that 6 years campaign a considerable number of sampling sites (62 snow-cores) were collected over this area with the majority over the Scandes. These snow-cores accounts for 45% of the total number of sample sites and their density can be characterized satisfactory with good overlap from year to year.

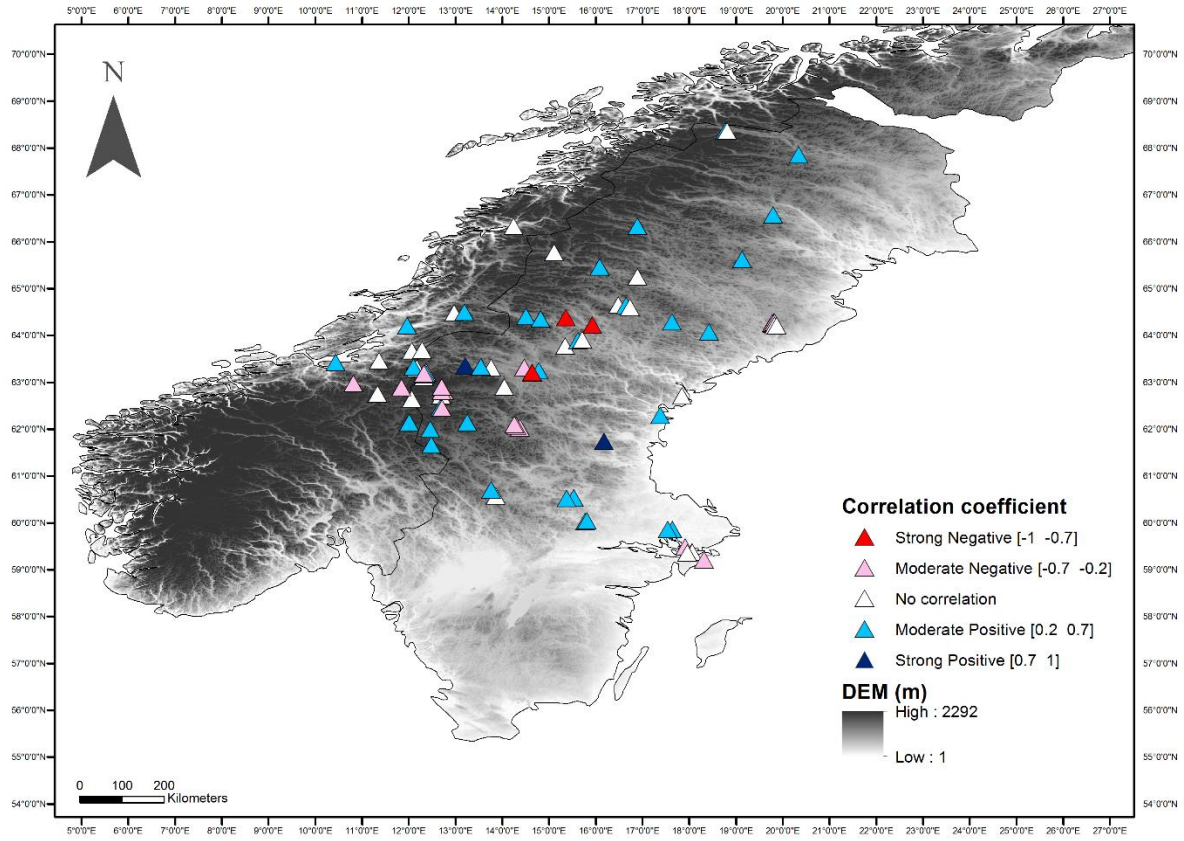

Figure 11: illustrates the outcome from the age-depth model. 143 snow-cores in 6 years campaign. Colorful triangles present the arithmitacally result of coefficient correlation R between $\delta^{18}O$ and the daily NAO. Reddish symbols are negative corralated area while bluish are areas with possetive correlation.Areas with white symbols are characterized as no-corelated.

Figure 12 illustrates the locations based on correlation coefficient 'R' between $\delta^{18}O$ and daily NAO. The presented sites are only 32 and this is because the *'no-correlated' 'm' areas* ($-0.2 < R < 0.2$) were removed. Table 1 lists analytical the geographical characteristic for each site and the respective correlation coefficient value. That table contains only the positive and negative correlated areas in central Scandinavia (same table pertaining to the overall extent are supplementary provided in appendix).

Table 1 : Sampling sites in central Scandinavia (study region) (without 'no correlated' sites). Geographic characteristics, correlation coefficient 'R' arithmetical and symbol, [1- (p value)] and related zone. Symbol is based on correlation coefficient scale which is stated in previous chapter.

Site-Name	Sampling Year	Latitude	Longitude	Elevation (m)	Correlation coefficient 'R'	Symbol	1 – (*p value)*	Zone
'ACC'	2015	61.990	12.462	581	0.38	y	0.68	3
'AR1'	2010	63.346	13.206	500	0.70	yy	0.97	1
'DT2'	2010	62.967	10.813	350	-0.24	n	0.55	2
'ELG1'	2015	62.135	12.006	890	0.26	y	0.63	3
'ELG2'	2015	61.657	12.485	800	0.33	y	0.84	3
'ELK01'	2013	64.347	14.823	294	0.51	y	0.84	1
'ELK02'	2013	64.347	14.823	294	0.66	y	0.96	1
'FAG1'	2012	64.402	14.503	360	0.25	y	0.51	1
'GET1'	2015	63.180	12.320	1100	-0.42	n	0.99	2
'GET3'	2014	63.174	12.314	875	-0.20	n	0.56	2
'GRO1'	2015	62.139	13.247	789	0.32	y	0.79	3
'GRO2'	2015	62.800	12.759	707	-0.21	n	0.54	2
'LJU1'	2011	62.440	12.708	574	-0.21	n	0.62	2
'LJU2'	2011	62.440	12.708	574	-0.20	n	0.39	2
'MA2'	2010	60.694	13.759	308	0.38	y	0.68	3
'MÖR1'	2011	63.325	13.537	355	0.23	y	0.55	1
'MÖR2'	2011	63.325	13.537	355	0.50	y	0.88	1
'NOS1'	2012	64.198	11.961	56	0.50	y	0.88	1
'NRG'	2014	62.885	11.842	775	-0.47	n	0.94	2
'NRG1'	2015	62.885	11.842	760	-0.30	n	0.77	2
'OS1'	2010	63.193	14.644	335	0.44	y	0.73	2
'OS2'	2010	63.239	14.783	382	0.49	y	0.74	2
'OS3'	2010	63.307	14.471	316	-0.25	n	0.46	2
'ÖST1'	2011	63.202	14.640	313	-0.50	n	0.97	2
'ÖST2'	2011	63.202	14.640	313	-0.80	nn	0.99	2
'SHJ01'	2013	63.217	12.364	950	-0.60	n	0.99	2
'SIB01'	2013	64.488	13.189	445	0.51	y	0.97	1
'SP3'	2012	63.151	12.350	783	-0.30	n	0.86	2
'ST1'	2010	63.317	12.098	630	0.35	y	0.90	1
'ST3'	2010	63.171	12.367	714	0.32	y	0.93	2
'SUA01'	2013	63.170	12.364	724	0.38	y	0.80	2
'SV1'	2010	62.025	14.378	350	-0.24	n	0.67	2
'SVE5'	2011	62.090	14.255	400	-0.26	n	0.47	2
'TA2'	2010	62.445	12.670	675	0.38	y	0.65	2
'TOR1'	2015	62.802	12.701	850	-0.41	n	0.87	2
'TOR2'	2015	62.890	12.701	833	-0.25	n	0.56	2
'TR1'	2010	63.416	10.434	118	0.56	y	0.81	1

'Quantitative approach' indicates almost a clear pattern for correlated (zone 1 and 3) or anti-correlated sites (zone 2). All northern sites (zone 1) are defined as positive correlated locations (blue triangles). These sites are located before the Scandes (looking from west to east) (e.g., *TR1-2010* and *SIB01- 2013*) or/and

their elevation is low (e.g., *ELK01-2013* = 294 m, *ELK02-2013* = 294 m and *FAG1-2012* = 360 m). Precipitation produced on Atlantic Ocean has not been affected by the Scandes yet. At the same time, a second zone ('negatively correlated') appears in the middle latitude sampling sites, on the top of the mountains. The majority of negatively correlated sites being affected by the high altitude. Bluish sites (bluish triangles) included in zone 2 but some of them have low [*1 - (p value)*] which may explain their behavior (e.g., *TA2-2010*). Changing the moist winds from Atlantic Ocean because of the Scandes can be related to these negative correlations (Uvo 2003a). Finally, the last zone (zone 3), in the south of the central Scandinavia, shows up again a positive correlation. The areas are detected on the Scandes foothills (South-East). Last zone areas (zone 3) are mostly influenced by easterly winds than westerly winds (Uvo 2003a), but in this analysis zone 3 locations are significantly correlated to the NAO index. (Different map is included in appendix for better understanding. Appendix. Figure 1 presents the site-names analytical).

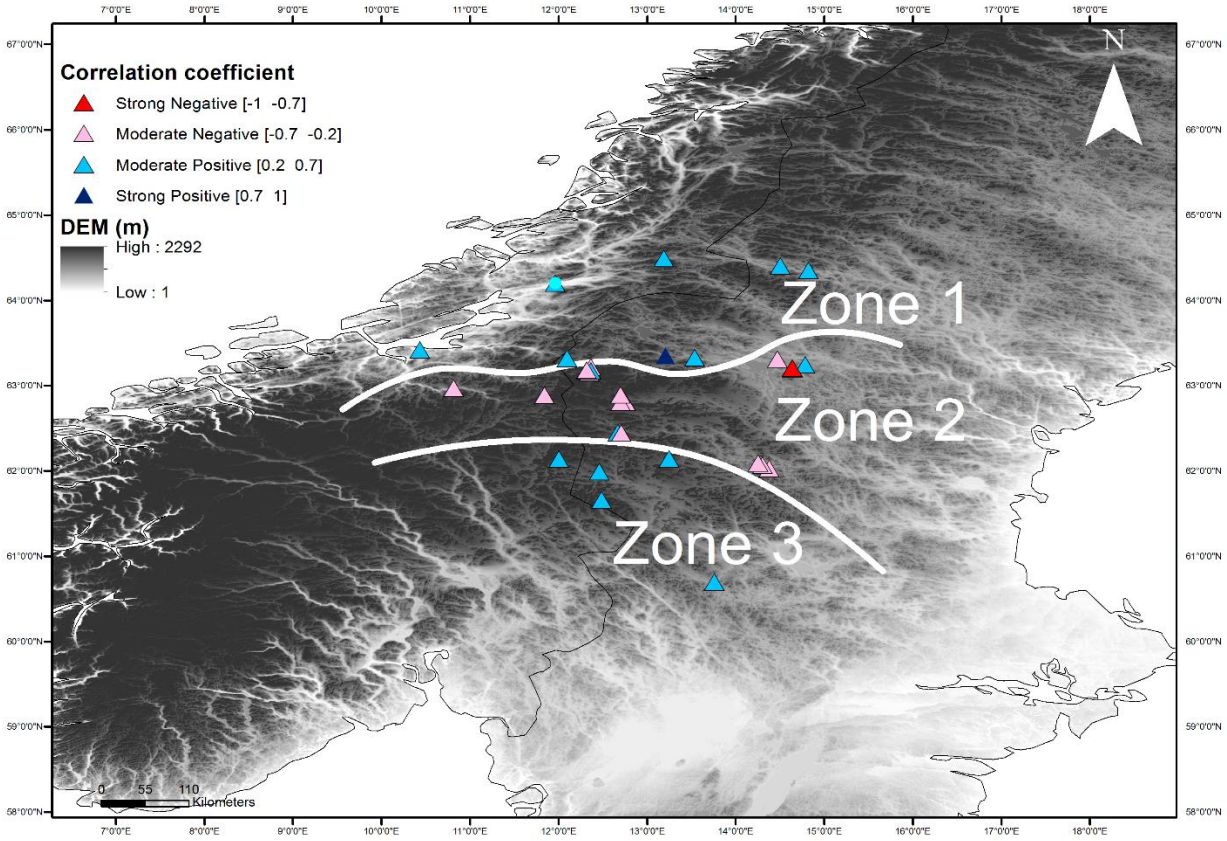

Figure 12: Central Scandinavia (study region). Colorful triangles present the arithmetical result of coefficient correlation R between $\delta^{18}O$ and the daily NAO index. Reddish symbols are negative correlated area while bluish are positive. 32 locations are visualized because 'no-correlated' records had been removed in order to highlight the patterns/zones.

4 Discussion

4.1 Age-depth Model/Algorithm

The age-depth model's performance is reasonable, thoughts for improvements can be suggested. The sampling protocol sets 5 cm depth for each slice in snow-core. Using that type of uniform-depth sampling, implies that we cannot relate all the isotopic signature to a unique date (daily NAO record) in case of heavy snowfall (exceeding 5 cm per day), the age-depth model will attribute several $\delta^{18}O$ values to the same date. On the other hand, in case of low snowfall, the $\delta^{18}O$ value attributed to a specific date will in fact a (precipitation-weighed) mean value for lumped time-interval needed for these 5 cm to get deposited. Therefore, the isotopic composition of each snow pack do not have to be correlated between daily records of NAO. For future projects, the correlation of each 5 centimeter snow-pack, it is more accurate to be between a mean values of daily NAO (precipitation-weighted NAO index). Those mean values should be described as time integrals between the considered and preceding date estimates (fig.13).

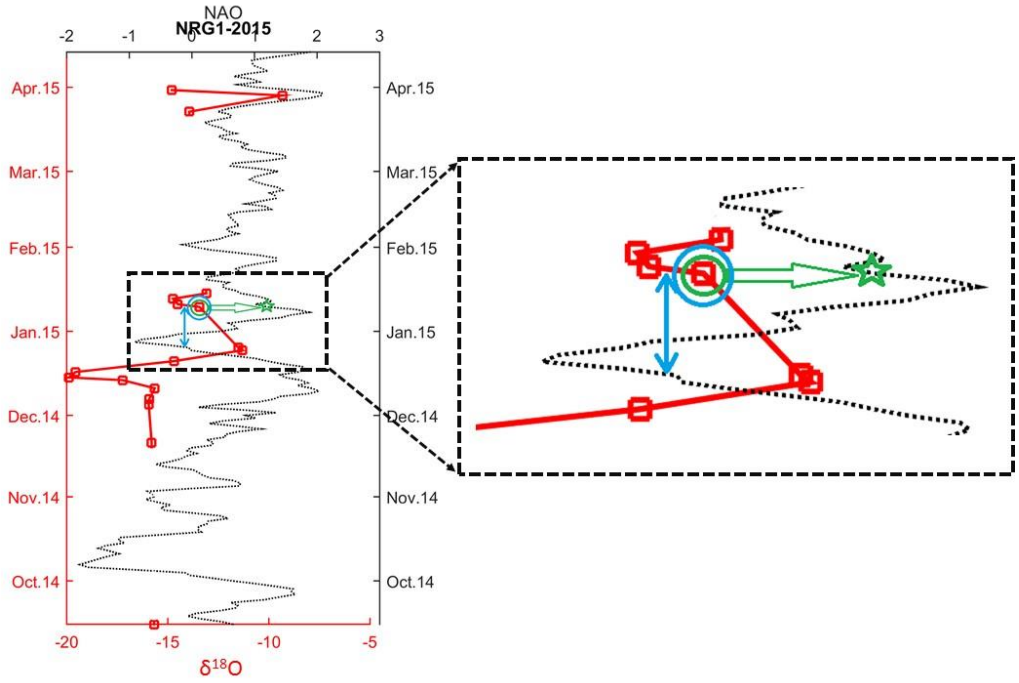

Figure 13: illustrates a possible future improvement for the algorithm. Green symbols show the current used values in order to calculate the correlation coefficient 'R' in this project. Green star presents the daily NAO's value, which is included in the calculation for correlation coefficient 'R'. Blue symbols recommend a better approach for future applications. Blue array explains the range of the days that can be used in order to have a mean daily NAO value. That blue array starts the next day of the previous record.

Moreover, the sampling location is another significant issue of the analysis. Age-depth profiles have more robust results in mid and high altitude areas (as confirmed on 'qualitative approach') because these locations receive on average a higher amount of snow, and are furthermore less subject to melting . If we

continue using the ERA Interim dataset for future analysis, we should avoid locations such as *VI1-2010*, *SVE3-2011* and *SVE5-2011* (fig.14).

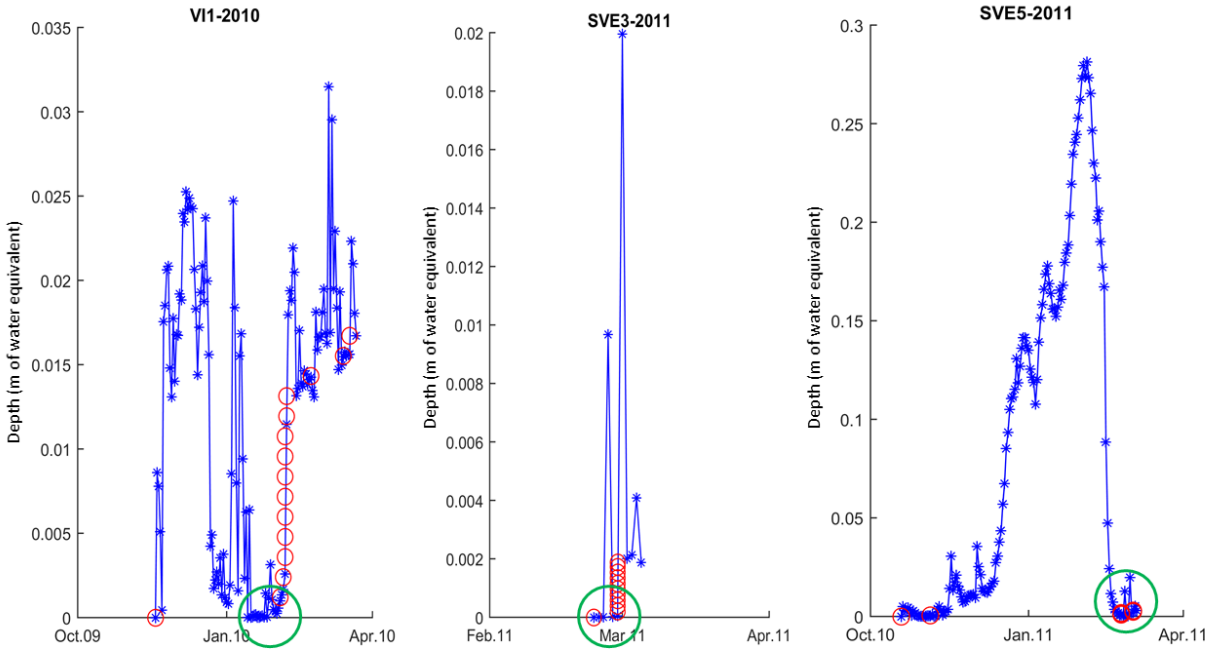

Figure 14: demonstrates age-depth model uncertainties based on low altitude areas. Intra-seasonal disappearance of snow-pack.

Figure 14 illustrates the abovementioned limitation. More precisely, the applied dataset contains some values corresponding to snow depth. The green cycles show the certain days with amounts of snow-depth close to but not exactly zero values. The *VI1-2010* could have the 'first day' of snow on 15th January instead of 20th November (in order to avoid producing gap from November to January). Also, areas without enough snowfalls must be neglected (*SVE3-2011* graph shows only 4 events). For a considered area and year (*SVE5-2011*) the maximum snow accumulation was in the middle of February. Fortunately for this research, all the outlined limitations addressed by choosing only central Scandinavia's (study region) snow-cores for further analysis.

An alternative, potentially complementary dating method would be to assign 'a priori' the same date to similar $\delta^{18}O$ extreme values found across nearby snow-cores. It can be assumed that individual isotopic signals (peak) relate to the same precipitation event. This approach will be analog to *wiggle matching* (W. Z Hoek 2001; Galimberti and Ramsey 2007). This proposal could me more effective if clouds or other meteorological variables could be inserted in the model to specify that 'grouped' areas.

Last but not least, the density profile of the snow-pack. ERA Interim dataset express snow depth (sd) in terms of water equivalent (m). For this thesis, the scaling of observed snow depth to *sd* (snow depth variable from ERA Interim dataset) became considering that the whole snow-core is uniform density. An

important extension of this analysis would be the integration of snow density, which should be born in mind for future campaigns. During previous campaigns, the density was measured constantly for non-fresh snow. These measurements gave an almost stable value (280 kg m^{-3}) for non-fresh snow which can be included in future analysis. Density's value combined with picture graphical assessment (fig. 4) (i.e. taking a picture of the core, to document snow characteristics, ice lenses etc.) from which we can separate fresh and non-fresh snow, will optimize our age-depth model. However, the picture optical assessment can be applied only for sampling with Russian corer because the sampling with shovel will not provide us with constant volume snow-pits. Characterizing the snow as fresh or non-fresh and measure the volume in situ can be a solution when the shovel is used.

4.2 Correlation NAO - $\delta^{18}O$ in central Sweden (study region)

Although, the proposed algorithm and the sampling protocol found application for first time, the results from 'quantitative approach' were able to exhibit the NAO's influence through central Scandinavia. Many reports mention that topography is not a main factor in controlling the climate (Brodie, Robertson, and Porter 1993; Timsic and Patterson 2014), while others state that the NAO maximizes its influences on mid to high latitudes (Hurrell et al. 2003a; Casado et al. 2013). That influence has been clarified focusing on that thesis on central Scandinavia.

The concept, to compare the NAO with the isotopic composition ($\delta^{18}O$) in each snow-core, is innovative, since never previously performed; following previous studies which had demonstrated relationship between precipitation's amount, temperature and the NAO (S. Brönnimann 2012). Uvo (2003) found evidence of the positive correlation between winter precipitation and the NAO index. Other studies indicate that snow-packs' isotopic signal write down every meteorological variations (Krinner et al. 1997; Steen-Larsen et al. 2011). Furthermore, long time series analysis (during the Holocene) emphasized the effect of the NAO to isotopic composition ($\delta^{18}O$) on precipitation over the central Sweden (St. Amour et al. 2010). Although, that paper based its results on lake-sediment cellulose and on high number of years, it was another incentive for this thesis. Summing up all the previous studies and applying the general theory on our data, have introduced an innovative approach for understanding the spatiotemporal NAO influences. The 6 years sampling and the spatial extent (100,000 km^2) of study area judged sufficient for a statistically significant analysis.

The findings of this study highlight zones of consistently positive/negative spatial correlation in central Scandinavia (Jämtland). These, however, could not be straightforward compared to previous studies due to the novelty of the proposed algorithm/protocol. These interpretations based on scientific reports which have demonstrated the correlation 'NAO - amount of precipitation' and 'NAO - spatial origin of precipitation'.

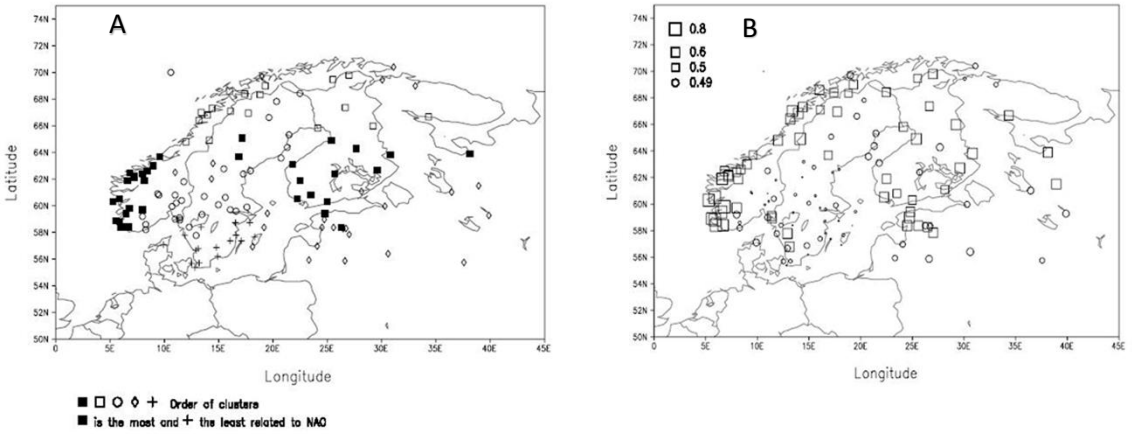

Figure 15: A. Results of cluster analysis on precipitation field. Different areas with similar precipitation variability are presented by different symbols (the rainfall stations were grouped according to their seasonal precipitation). This seasonal precipitation must have similar temporal variability. B. Correlation between the NAO index and seasonal precipitation totals. (The sizes of the symbols are analogous to correlation coefficient) (Source: Uvo 2003).

Spatial correlation was also found in Uvo (2003); a study that investigated the relationship between winter precipitation and the NAO over the central Scandinavia by performing cluster analysis on precipitation field (fig.15A). Indeed, similar patterns of clustering observed in this thesis. More specifically, areas with positive correlation (NAO - $\delta^{18}O$) over the study region (zone 1 and zone 3), align with the most correlated locations presented in figure 15A. In particular, the first zone is aligned with the clustering of squares (black or white) in the correlation map (fig.15A). And by transforming the symbolic scale to a numerical one (1 is +, 2 is ◊, 3 is O, 4 is □, 5 is ■), the cluster of squares stands for locations with correlation values of *5 and 4.* Our third zone, is aligned with the cluster where cycles are dominating (fig.15A) and those white cycles is translated to 3. The middle (second) zone characterized as 2 by Uvo (2003), 2 (◊) is the minimum correlation as far as central Sweden is concerned. Zone 2 in our study includes bluish triangles but it is good to mention that [*1 - (p value)*] can explain that result (sample sites with [*1 - (p value)*] < 0.70 present high probability of no-realistic result (R)). Areas such as *TA2-2010* (with [*1 - (p value)*] = 0.65) can be excluded from figure 12 and make the visualization more realistic and the zone 2 more homogenous according to correlation coefficient (R).

Moreover, the findings of this study are in good agreement with the patterns presented in figure 15B, where more correlated areas located westerly in Scandinavia. In these areas, precipitation events are coming from Atlantic Ocean, the clouds following winds direction (west to east) which have been generated by the different pressure between the Subpolar Low (Iceland) and the Subtropical High (Azores) (Greatbatch 2000). Analogous zones, based on precipitation fluctuation in Sweden, was also shown by (Busuioc, Chen, and Hellström 2001).

Another significant outcome that can be inferred from the abovementioned is that areas with positive correlation between the NAO and isotopic signal ($\delta^{18}O$) in snow-cores, ought to reveal a high proportion of correlation between the NAO and precipitation at the same time. On the other hand, negative correlated zones in our study might be expected to have a low proportion of correlation between the NAO

and precipitation. Such types of correlation adapt their magnitude temporally as a result of changing in the NAO's action centers (Casado et al. 2013).

4.3 Thoughts (Thesis Considerations) and future prospects

Different hypotheses, beyond these presented in this report, have been also investigated. Joel et al. (2001) related the altitude with the changes in water's isotopic composition. In our study using all (143) results from snow-cores, no significant correlation between the quantitative approach and the altitude observed. A reason of that, ought to be that our study includes only Scandinavia but Joel et al. (2001) refers the altitude as effect; while the $\delta^{18}O$ signature across the Scandes mainly reflects continental rainout.

Some other interpretations emerged from studies as (Visbeck et al. 2001; Lindström and Alexandersson 2004) and (Folland et al. 2009), who report the impact of the annual NAO to the Scandinavian climate. The thoughts guide us to examine the difference between the most positive phase NAO years and the most negative phase NAO years. In that campaign the most positive years are 2012 and 2015 and the most negative is 2010 (fig.1). However, no clear pattern emerged from the comparison of these extreme years in our dataset. A possible explanation might be that the data was too limited for this statistical approach due to the lack of samples (only 17 snow-cores are included in positive/negative correlated areas in 2012 and 2015).

It is beyond the scope of the present study to investigate an additional result from algorithm, hence we have not included in that project; the deuterium excess, which is a second order parameter. D_excess is a promising addition to first order $\delta^{18}O$-NAO analyses, because it integrates kinetic fractionation effect at the source region (Fujita and Abe 2006). Furthermore, the deuterium excess is related to surface temperature (Uemura et al. 2008; Sodemann and Zubler 2010) and local moisture (Pfahl and Sodemann 2014; Affolter et al. 2015). Temporal and spatial variations of the deuterium excess may produce considerable results in our area and it ought to be investigated in future reports.

There are several topics that could enhance the results presented in this thesis. The database used for the aim of this thesis consisted of 2415 snow-samples which are parts of 143 snow-cores over Sweden and central Norway, and thus can be a powerful tool for future scientific studies. Temperature and precipitation are another climate variables that will be investigated. Older reports have evaluated the influence of the NAO on areas' temperature (Langebroek, Werner, and Lohmann 2011; Pinto and Raible 2012; Casado et al. 2013). Jouzel (2003) characterized tracer of water cycle when isotopic signal ($\delta^{18}O$) is related to the temperature. The correlation between water stable isotopes and temperature have been referred as a factor for clarifying climate fluctuations and zones (Klein et al. 2015). Daily temperature can be also useful in order to address the precipitation-weighted temperature and for re-analysis data.

Extreme precipitation events are linked to the North Atlantic Oscillation (Serreze et al. 2000; Rigor, Wallace, and Colony 2002; Kevin Schaefer 2004). A possible analysis is if the unusual magnitude and/or the frequency of precipitation leave a signal to the water isotopic composition as Moreno et al. (2014) and Affolter et al. (2015) have suggested. Back-trajectories combination with precipitation might be useful to cluster locations and validate/improve the results. Furthermore, air parcels can be used backwards to identify the source of moisture since studies combine the variations in water isotopes with

the origin of moisture (Dansgaard 1964; Rozanski, Araguás-Araguás, and Gonfiantini 1993; Sodemann and Zubler 2010).

5 Conclusions

A new automated age-depth profile model is proposed, in which each specific date is attributed to 5 centimeters slice in every snow-core. The model offers a huge potential for many future projects since its script is structured to analyze sampling cores automatically. As with every model, limitations and uncertainties exist but improvements can be suggested after rigorous evaluation. In discussion chapter, a few suggestions for overcoming identified limitations have been introduced.

In addition to age-depth modelling part, the analysis describes the spatial and temporal variability of stable water isotopes in the snow pack and its relation to the NAO. That approach has developed in line with other abovementioned studies but centers on present (6 years) and not in the past. Fortunately, the results set the basis to start examining atmospheric phenomena in short time scale records and connecting them with their effects. It demonstrates that the NAO changes its phase the last 30 years and its impacts cannot be the same with those the previous years. Furthermore, it is significantly different to establish a project on sampling/real isotopic signatures instead of using data from other models. The previous denotation strengthens the short time scale approach. Achieving scientific significant conclusions in short term is more cost-effective and less time-consuming than spending 15 years on collecting data.

Besides the fact that the NAO's trend toward a positive phase is a new phenomenon and it is scientific significant to identify its effects, understanding its impacts and predict the future ones can be also evidenced a main factor for economic development in Scandinavia.

References

Affolter, Stéphane, Anamaria D. Häuselmann, Dominik Fleitmann, Philipp Häuselmann, and Markus Leuenberger. 2015. “Triple Isotope (δD, δ17O, δ18O) Study on Precipitation, Drip Water and Speleothem Fluid Inclusions for a Western Central European Cave (NW Switzerland).” *Quaternary Science Reviews*, Novel approaches to and new insights from speleothem-based climate reconstructions, 127 (November): 73–89. doi:10.1016/j.quascirev.2015.08.030.

Aggarwal, Pradeep K., Klaus Fröhlich, Kshitij M. Kulkarni, and Laurence L. Gourcy. 2004. “Stable Isotope Evidence for Moisture Sources in the Asian Summer Monsoon under Present and Past Climate Regimes.” *Geophysical Research Letters* 31 (8): L08203. doi:10.1029/2004GL019911.

Aizen, Vladimir B., Elena M. Aizen, Koji Fujita, Stanislav A. Nikitin, Karl J. Kreutz, and L. Nozomu Takeuchi. 2005. “Stable-Isotope Time Series and Precipitation Origin from Firn-Core and Snow Samples, Altai Glaciers, Siberia.” *Journal of Glaciology* 51 (175): 637–54.

Baldini, Lisa M., Frank McDermott, Aideen M. Foley, and James U. L. Baldini. 2008. “Spatial Variability in the European Winter Precipitation δ18O-NAO Relationship: Implications for Reconstructing NAO-Mode Climate Variability in the Holocene.” *Geophysical Research Letters* 35 (4): L04709. doi:10.1029/2007GL032027.

Bowen, Gabriel J., and Bruce Wilkinson. 2002. “Spatial Distribution of δ18O in Meteoric Precipitation.” *Geology* 30 (4): 315–18. doi:10.1130/0091-7613(2002)030<0315:SDOOIM>2.0.CO;2.

Brodie, George, Alexander Robertson, and Stuart Porter. 1993. *Climate and Weather of Newfoundland and Labrador*. Creative Book Publishing.

Busuioc, Aristita, Deliang Chen, and Cecilia Hellström. 2001. “Temporal and Spatial Variability of Precipitation in Sweden and Its Link with the Large-Scale Atmospheric Circulation.” *Tellus A* 53 (3): 348–67. doi:10.1034/j.1600-0870.2001.01152.x.

Casado, M., P. Ortega, V. Masson-Delmotte, C. Risi, D. Swingedouw, V. Daux, D. Genty, et al. 2013. “Impact of Precipitation Intermittency on NAO-Temperature Signals in Proxy Records.” *Clim. Past* 9 (2): 871–86. doi:10.5194/cp-9-871-2013.

Charles, C. D., D. Rind, J. Jouzel, R. D. Koster, and R. G. Fairbanks. 1994. “Glacial-Interglacial Changes in Moisture Sources for Greenland: Influences on the Ice Core Record of Climate.” *Science* 263 (5146): 508–11. doi:10.1126/science.263.5146.508.

Cook, Edward R. 2003. “Multi-Proxy Reconstructions of the North Atlantic Oscillation (NAO) Index: A Critical Review and a New Well-Verified Winter NAO Index Reconstruction Back to AD 1400.” In *The North Atlantic Oscillation: Climatic Significance and Environmental Impact*, edited by James W. Hurrell, Yochanan Kushnir, Geir Ottersen, and rtin Visbeck, 63–79. American Geophysical Union. http://onlinelibrary.wiley.com/doi/10.1029/134GM04/summary.

Dansgaard, W. 1964. “Stable Isotopes in Precipitation.” *Tellus* 16 (4): 436–68. doi:10.1111/j.2153-3490.1964.tb00181.x.

Darling, W. G. 2004. “Hydrological Factors in the Interpretation of Stable Isotopic Proxy Data Present and Past: A European Perspective.” *Quaternary Science Reviews*, Isotopes in Quaternary Paleoenvironmental reconstruction, 23 (7–8): 743–70. doi:10.1016/j.quascirev.2003.06.016.

Dee, D. P., S. M. Uppala, A. J. Simmons, P. Berrisford, P. Poli, S. Kobayashi, U. Andrae, et al. 2011. "The ERA-Interim Reanalysis: Configuration and Performance of the Data Assimilation System." *Quarterly Journal of the Royal Meteorological Society* 137 (656): 553–97. doi:10.1002/qj.828.

Dergachev, Valentin A., and Sergey S. Vasiliev. 2004. "Sources of δ18O Concentration Variability in Greenland Ice Cores: Temperature, North Atlantic Oscillation and Solar Activity." *Solar Physics* 224 (1-2): 433–43. doi:10.1007/s11207-005-8363-2.

Folland, Chris K., Jeff Knight, Hans W. Linderholm, David Fereday, Sarah Ineson, and James W. Hurrell. 2009. "The Summer North Atlantic Oscillation: Past, Present, and Future." *Journal of Climate* 22 (5): 1082–1103. doi:10.1175/2008JCLI2459.1.

Fujita, Koji, and Osamu Abe. 2006. "Stable Isotopes in Daily Precipitation at Dome Fuji, East Antarctica." *Geophysical Research Letters* 33 (18): L18503. doi:10.1029/2006GL026936.

Galimberti, Mariagrazia, and Christopher Bronk Ramsey. 2007. "Wiggle-Match Dating of Tree-Ring Sequences." *Radiocarbon* 46 (2): 917–24. doi:10.2458/azu_js_rc.46.4225.

Greatbatch, R. J. 2000. "The North Atlantic Oscillation." *Stochastic Environmental Research and Risk Assessment* 14 (4-5): 213–42. doi:10.1007/s004770000047.

Hammarlund, Dan, Lena Barnekow, H. J. B. Birks, Bjørn Buchardt, and Thomas W. D. Edwards. 2002. "Holocene Changes in Atmospheric Circulation Recorded in the Oxygen-Isotope Stratigraphy of Lacustrine Carbonates from Northern Sweden." *The Holocene* 12 (3): 339–51. doi:10.1191/0959683602hl548rp.

Harris, I., P.d. Jones, T.j. Osborn, and D.h. Lister. 2014. "Updated High-Resolution Grids of Monthly Climatic Observations – the CRU TS3.10 Dataset." *International Journal of Climatology* 34 (3): 623–42. doi:10.1002/joc.3711.

Hurrell, James W. 1996. "Influence of Variations in Extratropical Wintertime Teleconnections on Northern Hemisphere Temperature." *Geophysical Research Letters* 23 (6): 665–68. doi:10.1029/96GL00459.

Hurrell, James W., Yochanan Kushnir, Geir Ottersen, and Martin Visbeck. 2003a. "An Overview of the North Atlantic Oscillation." In *The North Atlantic Oscillation: Climatic Significance and Environmental Impact*, edited by James W. Hurrell, Yochanan Kushnir, Geir Ottersen, and rtin Visbeck, 1–35. American Geophysical Union. http://onlinelibrary.wiley.com/doi/10.1029/134GM01/summary.

Hurrell, James W., Yochanan Kushnir, Geir Ottersen, and Martin Visbeck 2003b. "An Overview of the North Atlantic Oscillation." In *The North Atlantic Oscillation: Climatic Significance and Environmental Impact*, edited by James W. Hurrell, Yochanan Kushnir, Geir Ottersen, and rtin Visbeck, 1–35. American Geophysical Union. http://onlinelibrary.wiley.com/doi/10.1029/134GM01/summary.

Hurrell, James W., and Harry Van Loon. 1997. "DECADAL VARIATIONS IN CLIMATE ASSOCIATED WITH THE NORTH ATLANTIC OSCILLATION." *Climatic Change* 36 (3-4): 301–26. doi:10.1023/A:1005314315270.

Insel, Nadja, Christopher J. Poulsen, Christophe Sturm, and Todd A. Ehlers. 2013. "Climate Controls on Andean Precipitation δ18O Interannual Variability." *Journal of Geophysical Research: Atmospheres* 118 (17): 9721–42. doi:10.1002/jgrd.50619.

Joel et al. 2001. "Environmental Isotopes in the Hydrological Cycle Vol 2."

Jones, Philip D., Timothy J. Osborn, and Keith R. Briffa. 2003. “Pressure-Based Measures of the North Atlantic Oscillation (NAO): A Comparison and an Assessment of Changes in the Strength of the NAO and in Its Influence on Surface Climate Parameters.” In *The North Atlantic Oscillation: Climatic Significance and Environmental Impact*, edited by James W. Hurrell, Yochanan Kushnir, Geir Ottersen, and rtin Visbeck, 51–62. American Geophysical Union. http://onlinelibrary.wiley.com/doi/10.1029/134GM03/summary.

Jouzel, J. 2003. “Water Stable Isotopes: Atmospheric Composition and Applications in Polar Ice Core Studies.” *Treatise on Geochemistry* 4 (December): 213–43. doi:10.1016/B0-08-043751-6/04040-8.

Kevin Schaefer, A. Scott Denning. 2004. “The Winter Arctic Oscillation and the Timing of Snowmelt in Europe. Geophys Res Lett.” *Geophysical Research Letters - GEOPHYS RES LETT* 31 (22). doi:10.1029/2004GL021035.

Klein, E.s., M. Nolan, J. McConnell, M. Sigl, J. Cherry, J. Young, and J.m. Welker. 2015. “McCall Glacier Record of Arctic Climate Change: Interpreting a Northern Alaska Ice Core with Regional Water Isotopes.” *Quaternary Science Reviews*, July. doi:10.1016/j.quascirev.2015.07.030.

Kress, Anne, Matthias Saurer, Rolf T. W. Siegwolf, David C. Frank, Jan Esper, and Harald Bugmann. 2010. “A 350 Year Drought Reconstruction from Alpine Tree Ring Stable Isotopes.” *Global Biogeochemical Cycles* 24 (2): GB2011. doi:10.1029/2009GB003613.

Krinner, Gerhard, Christophe Genthon, Zhao-Xin Li, and Phu Le Van. 1997. “Studies of the Antarctic Climate with a Stretched-Grid General Circulation Model.” *Journal of Geophysical Research: Atmospheres* 102 (D12): 13731–45. doi:10.1029/96JD03356.

Labuhn, Inga, Dominique Genty, Hubert Vonhof, Clément Bourdin, Dominique Blamart, Eric Douville, Jiaoyang Ruan, et al. 2015. “A High-Resolution Fluid Inclusion δ18O Record from a Stalagmite in SW France: Modern Calibration and Comparison with Multiple Proxies.” *Quaternary Science Reviews* 110 (February): 152–65. doi:10.1016/j.quascirev.2014.12.021.

Langebroek, P. M., M. Werner, and G. Lohmann. 2011. “Climate Information Imprinted in Oxygen-Isotopic Composition of Precipitation in Europe.” *Earth and Planetary Science Letters* 311 (1–2): 144–54. doi:10.1016/j.epsl.2011.08.049.

Lindström, Göran, and Hans Alexandersson. 2004. “Recent Mild and Wet Years in Relation to Long Observation Records and Future Climate Change in Sweden.” *Ambio* 33 (4-5): 183–86.

Liu, Zhongfang, Kei Yoshimura, Gabriel J. Bowen, Nikolaus H. Buenning, Camille Risi, Jeffrey M. Welker, and Fasong Yuan. 2014. “Paired Oxygen Isotope Records Reveal Modern North American Atmospheric Dynamics during the Holocene.” *Nature Communications* 5 (April): 3701. doi:10.1038/ncomms4701.

McDermott, Frank. 2004. “Palaeo-Climate Reconstruction from Stable Isotope Variations in Speleothems: A Review.” *Quaternary Science Reviews*, Isotopes in Quaternary Paleoenvironmental reconstruction, 23 (7–8): 901–18. doi:10.1016/j.quascirev.2003.06.021.

Merlivat, Liliane, and Jean Jouzel. 1979. “Global Climatic Interpretation of the Deuterium-Oxygen 18 Relationship for Precipitation.” *Journal of Geophysical Research: Oceans* 84 (C8): 5029–33. doi:10.1029/JC084iC08p05029.

Moreno, Ana, Carlos Sancho, Miguel Bartolomé, Belén Oliva-Urcia, Antonio Delgado-Huertas, Mª Estrela, David Corell, Juan López-Moreno, and Isabel Cacho. 2014. “Climate Controls on Rainfall Isotopes

and Their Effects on Cave Drip Water and Speleothem Growth: The Case of Molinos Cave (Teruel, NE Spain)." *Climate Dynamics* 43 (1/2): 221–41. doi:10.1007/s00382-014-2140-6.

Osborn, T. J., K. R. Briffa, S. F. B. Tett, P. D. Jones, and R. M. Trigo. 1999. "Evaluation of the North Atlantic Oscillation as Simulated by a Coupled Climate Model." *Climate Dynamics* 15 (9): 685–702. doi:10.1007/s003820050310.

Petit, J. R., J. Jouzel, D. Raynaud, N. I. Barkov, J.-M. Barnola, I. Basile, M. Bender, et al. 1999. "Climate and Atmospheric History of the Past 420,000 Years from the Vostok Ice Core, Antarctica." *Nature* 399 (6735): 429–36. doi:10.1038/20859.

Pfahl, S., and H. Sodemann. 2014. "What Controls Deuterium Excess in Global Precipitation?" *Clim. Past* 10 (2): 771–81. doi:10.5194/cp-10-771-2014.

Pinto, Joaquim G., and Christoph C. Raible. 2012. "Past and Recent Changes in the North Atlantic Oscillation." *Wiley Interdisciplinary Reviews: Climate Change* 3 (1): 79–90. doi:10.1002/wcc.150.

Rigor, Ignatius G., John M. Wallace, and Roger L. Colony. 2002. "Response of Sea Ice to the Arctic Oscillation." *Journal of Climate* 15 (18): 2648–63. doi:10.1175/1520-0442(2002)015<2648:ROSITT>2.0.CO;2.

Rosqvist, Gunhild C., Melanie J. Leng, Tomasz Goslar, Hilary J. Sloane, Christian Bigler, Laura Cunningham, Anna Dadal, et al. 2013. "Shifts in Precipitation during the Last Millennium in Northern Scandinavia from Lacustrine Isotope Records." *Quaternary Science Reviews*, International Association of Limnogeology – Isotopes and Lakes, 66 (April): 22–34. doi:10.1016/j.quascirev.2012.10.030.

Rozanski, Kazimierz, Luis Araguás-Araguás, and Roberto Gonfiantini. 1993. "Isotopic Patterns in Modern Global Precipitation." In *Climate Change in Continental Isotopic Records*, edited by P. K. Swart, K. C. Lohmann, J. Mckenzie, and S. Savin, 1–36. American Geophysical Union. http://onlinelibrary.wiley.com/doi/10.1029/GM078p0001/summary.

S. Brönnimann, I. Mariani. 2012. "Simulating the Temperature and Precipitation Signal in an Alpine Ice Core." *Climate of the Past Discussions* 8 (6): 6111–34. doi:10.5194/cpd-8-6111-2012.

Seager, Richard, Yochanan Kushnir, Martin Visbeck, Naomi Naik, Jennifer Miller, Gerd Krahmann, and Heidi Cullen. 2000. "Causes of Atlantic Ocean Climate Variability between 1958 and 1998*." *Journal of Climate* 13 (16): 2845–62. doi:10.1175/1520-0442(2000)013<2845:COAOCV>2.0.CO;2.

Serreze, M. C., J. E. Walsh, F. S. Chapin Iii, T. Osterkamp, M. Dyurgerov, V. Romanovsky, W. C. Oechel, J. Morison, T. Zhang, and R. G. Barry. 2000. "Observational Evidence of Recent Change in the Northern High-Latitude Environment." *Climatic Change* 46 (1-2): 159–207. doi:10.1023/A:1005504031923.

Sjolte, J., G. Hoffmann, S. J. Johnsen, B. M. Vinther, V. Masson-Delmotte, and C. Sturm. 2011. "Modeling the Water Isotopes in Greenland Precipitation 1959–2001 with the Meso-Scale Model REMO-Iso." *Journal of Geophysical Research: Atmospheres* 116 (D18): D18105. doi:10.1029/2010JD015287.

Sodemann, H., and E. Zubler. 2010. "Seasonal and Inter-Annual Variability of the Moisture Sources for Alpine Precipitation during 1995-2002." *International Journal of Climatology* 30 (7): 947–61. doi:10.1002/joc.1932.

St. Amour, Natalie A., Dan Hammarlund, Thomas W.d. Edwards, and Brent B. Wolfe. 2010. "New Insights into Holocene Atmospheric Circulation Dynamics in Central Scandinavia Inferred from Oxygen-

Isotope Records of Lake-Sediment Cellulose." *Boreas* 39 (4): 770–82. doi:10.1111/j.1502-3885.2010.00169.x.

Steen-Larsen, Hc, V Masson-Delmotte, J Sjolte, Sj Johnsen, Bm Vinther, Fm Breon, Hb Clausen, et al. 2011. "Understanding the Climatic Signal in the Water Stable Isotope Records from the NEEM Shallow Firn/ice Cores in Northwest Greenland." *JOURNAL OF GEOPHYSICAL RESEARCH-ATMOSPHERES* 116 (March).

Straile, Dietmar, David M. Livingstone, Gesa A. Weyhenmeyer, and D. Glen George. 2003. "The Response of Freshwater Ecosystems to Climate Variability Associated with the North Atlantic Oscillation." In *The North Atlantic Oscillation: Climatic Significance and Environmental Impact*, edited by James W. Hurrell, Yochanan Kushnir, Geir Ottersen, and rtin Visbeck, 263–79. American Geophysical Union. http://onlinelibrary.wiley.com/doi/10.1029/134GM12/summary.

Sturm, C., Q. Zhang, and D. Noone. 2010. "An Introduction to Stable Water Isotopes in Climate Models: Benefits of Forward Proxy Modelling for Paleoclimatology." *Clim. Past* 6 (1): 115–29. doi:10.5194/cp-6-115-2010.

Thompson, Lonnie G., Ellen Mosley-Thompson, M. E. Davis, P.-N. Lin, K. Henderson, and T. A. Mashiotta. 2003. "Tropical Glacier and Ice Core Evidence of Climate Change on Annual to Millennial Time Scales." *Climatic Change* 59 (1-2): 137–55. doi:10.1023/A:1024472313775.

Tian, Lide, Tandong Yao, Zhen Li, Kenneth MacClune, Guangjian Wu, Baiqing Xu, Yuefang Li, Anxian Lu, and Yongping Shen. 2006. "Recent Rapid Warming Trend Revealed from the Isotopic Record in Muztagata Ice Core, Eastern Pamirs." *Journal of Geophysical Research: Atmospheres* 111 (D13): D13103. doi:10.1029/2005JD006249.

Timsic, Sandra, and William P. Patterson. 2014. "Spatial Variability in Stable Isotope Values of Surface Waters of Eastern Canada and New England." *Journal of Hydrology* 511 (April): 594–604. doi:10.1016/j.jhydrol.2014.02.017.

Uemura, Ryu, Yohei Matsui, Kei Yoshimura, Hideaki Motoyama, and Naohiro Yoshida. 2008. "Evidence of Deuterium Excess in Water Vapor as an Indicator of Ocean Surface Conditions." *Journal of Geophysical Research: Atmospheres* 113 (D19): D19114. doi:10.1029/2008JD010209.

Uvo, Cintia B. 2003a. "Analysis and Regionalization of Northern European Winter Precipitation Based on Its Relationship with the North Atlantic Oscillation." *International Journal of Climatology* 23 (10): 1185–94. doi:10.1002/joc.930.

Uvo, Cintia B.. 2003b. "Analysis and Regionalization of Northern European Winter Precipitation Based on Its Relationship with the North Atlantic Oscillation." *International Journal of Climatology* 23 (10): 1185–94. doi:10.1002/joc.930.

Vinther, B. M., K. K. Andersen, P. D. Jones, K. R. Briffa, and J. Cappelen. 2006. "Extending Greenland Temperature Records into the Late Eighteenth Century." *Journal of Geophysical Research (Atmospheres)* 111 (June): D11105. doi:10.1029/2005JD006810.

Visbeck, M. H., J. W. Hurrell, L. Polvani, and H. M. Cullen. 2001. "The North Atlantic Oscillation: Past, Present, and Future." *Proceedings of the National Academy of Sciences of the United States of America* 98 (23): 12876–77. doi:10.1073/pnas.231391598.

Wanner, Heinz, Stefan Brönnimann, Carlo Casty, Dimitrios Gyalistras, Jürg Luterbacher, Christoph Schmutz, David B. Stephenson, and Eleni Xoplaki. 2001. "North Atlantic Oscillation – Concepts And Studies." *Surveys in Geophysics* 22 (4): 321–81. doi:10.1023/A:1014217317898.

Welker, Jeffrey M., Shelly Rayback, and Greg H . R. Henry. 2005. “Arctic and North Atlantic Oscillation Phase Changes Are Recorded in the Isotopes (δ18O and δ13C) of Cassiope Tetragona Plants.” *Global Change Biology* 11 (7): 997–1002. doi:10.1111/j.1365-2486.2005.00961.x.

Werner, Martin, Uwe Mikolajewicz, Martin Heimann, and Georg Hoffmann. 2000. “Borehole versus Isotope Temperatures on Greenland: Seasonality Does Matter.” *Geophysical Research Letters* 27 (5): 723–26. doi:10.1029/1999GL006075.

White, J. W. C., L. K. Barlow, D. Fisher, P. Grootes, J. Jouzel, S. J. Johnsen, M. Stuiver, and H. Clausen. 1997. “The Climate Signal in the Stable Isotopes of Snow from Summit, Greenland: Results of Comparisons with Modern Climate Observations.” *Journal of Geophysical Research: Oceans* 102 (C12): 26425–39. doi:10.1029/97JC00162.

W. Z Hoek, S. J. P. Bohncke. 2001. “Oxygen-Isotope Wiggle Matching as a Tool for Synchronising Ice-Core and Terrestrial Records over Termination 1.” *Quaternary Science Reviews* 20 (11): 1251–64. doi:10.1016/S0277-3791(00)00150-5.

Appendix

Table 1: All ice cores 143. Geographic characteristics, qualitative approach as described in methods, correlation coefficient 'R' arithmetical and symbolism between the daily NAO and $\delta^{18}O$ and correlation coefficient 'R' arithmetical and symbolism between the daily NAO and deuterium excess. Symbolism is based on correlation coefficient scale which has been stated in results chapter.

Site Name	Year	Latitude	Longitude	Elevation (m)	'Qualitative correlation' NAO - $\delta^{18}O$ Symbolism	' Quantitative correlation' NAO - $\delta^{18}O$ Correlation coefficient 'R'	' Quantitative correlation' NAO - $\delta^{18}O$ Symbolism	' Quantitative correlation' NAO - deuterium excess Correlation coefficient 'R'	' Quantitative correlation' NAO - deuterium excess Symbolism
'AR1'	2010	63.346	13.206	500	y	0.70	yy	-0.45	n
'AR2'	2010	63.313	13.761	336	y	0.19	m	0.04	m
'BO1'	2010	60.528	15.531	120	y	0.68	y	0.27	y
'BO2'	2010	60.528	15.531	120	y	0.64	y	0.44	y
'BO3'	2010	60.517	15.376	158	y	0.68	y	-0.21	n
'BR1'	2010	63.882	15.619	308	m	0.30	y	0.76	yy
'BR2'	2010	63.902	15.710	291	m	-0.07	m	0.32	y
'DT1'	2010	62.642	12.060	840	n	0.05	m	-0.39	n
'DT2'	2010	62.967	10.813	350	n	-0.24	n	0.01	m
'DU1'	2010	64.074	18.423	307	y	0.21	y	-0.23	n
'FA1'	2010	60.017	15.768	124	y	0.73	yy	0.28	y
'FA2'	2010	60.017	15.768	124	y	0.60	y	0.15	m
'FA3'	2010	60.032	15.807	147	m	0.48	y	0.23	y
'KR1'	2010	64.255	19.780	259	n	-0.27	n	0.24	y
'KR10'	2010	64.199	19.870	157	n	-0.42	n	0.05	m
'KR11'	2010	64.245	19.770	231	m	0.02	m	0.10	m
'KR12'	2010	64.245	19.770	231	m	0.06	m	0.05	m
'KR13'	2010	64.245	19.770	231	m	0.04	m	0.00	m
'KR2'	2010	64.255	19.780	259	n	-0.56	n	0.31	y
'KR3'	2010	64.255	19.780	259	n	-0.16	m	0.35	y
'KR4'	2010	64.255	19.780	259	n	-0.51	n	0.36	y
'KR5'	2010	64.273	19.826	301	m	-0.23	n	0.12	m
'KR6'	2010	64.273	19.826	301	n	-0.29	n	0.61	y
'KR7'	2010	64.208	19.826	219	n	-0.15	m	0.09	m
'KR8'	2010	64.208	19.826	219	n	-0.19	m	0.16	m
'KR9'	2010	64.199	19.870	157	n	-0.19	m	0.34	y
'MA1'	2010	60.694	13.759	308	m	-0.01	m	-0.78	nn

'MA2'	2010	60.694	13.759	308	y	0.38	y	-0.79	nn
'MA3'	2010	60.566	13.860	323	m	0.00	m	-0.61	n
'OS1'	2010	63.193	14.644	335	y	0.44	y	-0.17	m
'OS2'	2010	63.239	14.783	382	y	0.49	y	0.37	y
'OS3'	2010	63.307	14.471	316	m	-0.25	n	0.62	y
'ROT1'	2010	59.481	17.909	4	y	-0.33	n	-0.06	m
'ST1'	2010	63.317	12.098	630	m	0.35	y	-0.47	n
'ST2'	2010	63.297	12.167	637	m	-0.03	m	-0.04	m
'ST3'	2010	63.171	12.367	714	y	0.32	y	-0.51	n
'ST4'	2010	63.190	12.386	725	m	-0.06	m	0.05	m
'STO1'	2010	59.369	18.059	13	y	-0.38	n	-0.03	m
'STO2'	2010	59.364	18.065	16	y	0.14	m	-0.14	m
'STO2B'	2010	59.364	18.065	16	y	-0.09	m	0.44	y
'STO3'	2010	59.347	17.958	18	y	0.20	y	-0.19	m
'STO4'	2010	59.209	18.313	1	y	-0.33	n	0.24	y
'STO5'	2010	59.347	17.958	18	y	-0.19	m	-0.23	n
'SUN'	2010	62.290	17.378	2	m	0.63	y	-0.76	nn
'SV1'	2010	62.025	14.378	350	n	-0.24	n	-0.48	n
'TA1'	2010	62.442	12.686	733	m	-0.08	m	-0.76	nn
'TA2'	2010	62.445	12.670	675	y	0.38	y	-0.62	n
'TA3'	2010	62.442	12.674	675	y	0.19	m	-0.72	nn
'TR1'	2010	63.416	10.434	118	m	0.56	y	-0.58	n
'TS'	2010	63.458	11.359	260	m	-0.16	m	-0.32	n
'UP1'	2010	59.849	17.635	13	y	0.28	y	-0.21	n
'UP2'	2010	59.849	17.635	13	y	0.32	y	-0.12	n
'UP3'	2010	59.850	17.536	33	y	0.53	y	-0.44	n
'VI1'	2010	64.633	16.644	391	m	0.40	y	-0.33	n
'VI2'	2010	64.600	16.731	361	n	0.07	m	0.22	y
'ABI1'	2011	66.323	16.890	630	y	0.03	m	0.29	y
'ABI1B'	2011	68.362	18.774	376	y	-0.02	m	0.90	yy
'ABI1C'	2011	68.362	18.774	376	y	0.14	m	0.45	y
'ABI2'	2011	66.323	16.890	630	y	-0.06	m	0.59	y
'ABI2B'	2011	68.362	18.774	376	y	0.44	y	-0.03	m
'ABI5'	2011	68.355	18.809	361	y	-0.06	m	0.69	y
'ARV1'	2011	65.619	19.128	354	y	0.59	y	-0.11	m
'ARV2'	2011	65.619	19.128	354	y	0.50	y	0.14	m
'BLA1'	2011	65.246	16.890	421	y	0.25	y	-0.14	m
'BLA2'	2011	65.246	16.890	421	y	0.19	m	-0.09	m
'HAL1'	2011	63.764	15.346	357	m	-0.34	n	0.08	m
'HAL2'	2011	63.764	15.346	357	m	-0.50	n	-0.02	m
'HAL5'	2011	63.764	15.346	357	y	-0.10	m	-0.07	m
'HEM1'	2011	65.771	15.112	493	y	0.57	y	-0.38	n
'HEM2'	2011	65.771	15.112	493	y	x	NaN	x	NaN

'JOK1'	2011	66.566	19.789	337	m	0.32	y	0.58	y
'JOK2'	2011	66.566	19.789	337	n	0.51	y	0.31	y
'KIR1'	2011	67.846	20.340	441	y	0.27	y	-0.18	m
'KRY1'	2011	64.282	19.812	282	m	-0.18	m	0.53	y
'KRY2'	2011	64.282	19.812	282	m	0.33	y	0.40	y
'KRY4'	2011	64.255	19.780	259	m	0.07	m	0.52	y
'KRY5'	2011	64.255	19.780	259	y	0.29	y	0.35	y
'LAX1'	2011	64.642	16.479	351	y	0.53	y	-0.22	n
'LAX2'	2011	64.642	16.479	351	m	0.06	m	0.55	y
'LJU1'	2011	62.440	12.708	574	n	-0.21	n	0.12	m
'LJU2'	2011	62.440	12.708	574	y	-0.20	n	-0.44	n
'MOI1'	2011	66.323	14.237	30	y	0.11	m	0.11	m
'MOI2'	2011	66.323	16.890	630	y	0.48	y	-0.10	m
'MÖR1'	2011	63.325	13.537	355	y	0.23	y	0.17	m
'MÖR2'	2011	63.325	13.537	355	y	0.50	y	0.06	m
'NOR1'	2011	65.461	16.085	420	y	0.49	y	0.05	m
'NOR2'	2011	65.461	16.085	420	y	0.45	y	-0.05	m
'NOR5'	2011	65.461	16.085	420	y	0.28	y	0.10	m
'ÖST1'	2011	63.202	14.640	313	m	-0.50	n	0.20	y
'ÖST2'	2011	63.202	14.640	313	n	-0.80	nn	0.25	y
'SJA1'	2011	62.697	17.845	46	m	-0.21	n	-0.46	n
'SJA2'	2011	62.697	17.845	46	y	x	NaN	x	NaN
'STR1'	2011	63.166	12.336	793	n	-0.10	m	0.31	y
'STR2'	2011	63.166	12.336	793	n	-0.18	m	0.10	m
'SVE2'	2011	62.062	14.303	400	m	x	NaN	x	NaN
'SVE3'	2011	62.062	14.303	400	m	-0.41	n	0.62	y
'SVE5'	2011	62.090	14.255	400	n	-0.26	n	0.78	yy
'TRO1'	2011	62.744	11.329	700	y	x	NaN	x	x
'ADV1'	2012	63.666	12.061	340	n	0.13	m	0.56	y
'ADV3'	2012	63.686	12.286	508	n	x	NaN	x	NaN
'FAG1'	2012	64.402	14.503	360	m	0.25	y	-0.03	m
'FAN1'	2012	64.374	15.363	440	m	-0.27	n	0.06	m
'KRY1'	2012	64.245	19.771	231	y	-0.07	m	0.29	y
'KRY11'	2012	64.234	19.787	197	y	x	NaN	x	NaN
'KRY3'	2012	64.245	19.772	231	m	0.23	y	0.43	y
'KRY5'	2012	64.255	19.785	279	m	0.39	y	-0.08	m
'KRY7'	2012	64.255	19.785	279	m	0.33	y	-0.17	m
'KRY9'	2012	64.234	19.787	197	y	0.75	yy	-0.41	n
'NOS1'	2012	64.198	11.961	56	y	0.50	y	-0.58	n
'SIB1'	2012	64.472	12.971	340	y	x	NaN	x	NaN
'SP1'	2012	63.107	12.324	896	m	x	NaN	x	NaN
'SP3'	2012	63.151	12.350	783	m	-0.30	n	-0.03	m
'ELK01'	2013	64.347	14.823	294	m	0.51	y	-0.30	n

'ELK02'	2013	64.347	14.823	294	m	0.66	y	-0.18	m
'JAR1'	2013	61.736	16.171	110	m	0.80	yy	-0.95	nn
'KRY01'	2013	64.253	19.785	279	m	0.25	y	-0.05	m
'KRY02'	2013	64.255	19.783	279	y	0.33	y	-0.02	m
'KRY03'	2013	64.245	19.771	231	y	0.45	y	0.14	m
'KRY04'	2013	64.245	19.771	231	y	0.26	y	0.03	m
'KRY05'	2013	64.245	19.771	231	y	0.60	y	-0.29	n
'KYR'	2013	64.217	15.925	312	m	-0.82	nn	0.56	y
'SHJ01'	2013	63.217	12.364	950	n	-0.60	n	-0.21	n
'SIB01'	2013	64.488	13.189	445	m	0.51	y	0.19	m
'SUA01'	2013	63.170	12.364	724	y	0.38	y	-0.20	n
'TBG'	2013	64.287	17.631	389	m	0.50	y	-0.28	n
'DUM'	2014	62.706	12.694	819	m	0.08	m	-0.08	m
'GET1'	2014	63.188	12.369	730	n	0.06	m	0.08	m
'GET2'	2014	63.189	12.367	730	n	-0.17	m	-0.41	n
'GET3'	2014	63.174	12.314	875	m	-0.20	n	-0.46	n
'NRG'	2014	62.885	11.842	775	y	-0.47	n	-0.31	n
'SUF'	2014	63.169	12.363	724	n	-0.09	m	0.08	m
'SUN'	2014	62.893	14.043	620	y	0.09	m	0.01	m
'TOR1'	2014	62.890	12.701	833	n	0.12	m	0.14	m
'ACC'	2015	61.990	12.462	581	y	0.38	y	-0.65	n
'ELG1'	2015	62.135	12.006	890	y	0.26	y	-0.23	n
'ELG2'	2015	61.657	12.485	800	m	0.33	y	-0.57	n
'GET1'	2015	63.180	12.320	1100	n	-0.42	n	-0.13	m
'GRO1'	2015	62.139	13.247	789	m	0.32	y	-0.46	n
'GRO2'	2015	62.800	12.759	707	n	-0.21	n	-0.51	n
'NRG1'	2015	62.885	11.842	760	n	-0.30	n	-0.17	m
'SUF'	2015	63.168	12.360	724	m	0.16	m	0.35	y
'TOR1'	2015	62.802	12.701	850	n	-0.41	n	-0.53	n
'TOR2'	2015	62.890	12.701	833	n	-0.25	n	0.29	y

Table 2: Matlab Algorithm.

```
clear all
close all
clc

%%
fileID =fopen('f_total_cores.txt');


C = textscan(fileID,'%f %s %q %s %f %f %f %f %f %f %f %f %f %q');
fclose(fileID);
```

```
celldisp(C);

C_cols={'ID_num','ID_str','Site','Slice','Lat','Lon',...
    'X','Y','Depth','Dens','d18O','dD','Year','Date'};
C_struct=cell2struct(C,C_cols,2);

ind_profile=regexp(C_struct.Slice,'^S','start');
ind_profile=~cellfun(@isempty,ind_profile);
ind_nfresh=~strcmp('FRESH',C_struct.Site);
ind_profile=ind_profile & ind_nfresh;

C_profile=structfun(@(vec) vec(ind_profile),C_struct,'UniformOutput',false);
C_profile.SiteYear=cellfun(...
    @(sit,yr) sprintf('%s-%i',sit,yr),...
    C_profile.Site,num2cell(C_profile.Year),...
    'UniformOutput',false);
C_profile.d18O(C_profile.d18O<=-998)=NaN;
C_profile.dD(C_profile.dD<=-998)=NaN;

s=unique(C_profile.SiteYear,'stable');

 for a=1:length(b);

    ind = strcmp(s,C_profile.SiteYear);

    CORE_struct(a).Site=unique(C_profile.Site(ind));
    CORE_struct(a).Year=unique(C_profile.Year(ind));
    CORE_struct(a).Date=unique(C_profile.Date(ind));
    CORE_struct(a).Lon=unique(C_profile.Lon(ind));
    CORE_struct(a).Lat=unique(C_profile.Lat(ind));
    CORE_struct(a).ind=ind;
    CORE_struct(a).Depth=C_profile.Depth(ind);
    CORE_struct(a).d18O=C_profile.d18O(ind);
    CORE_struct(a).dD=C_profile.dD(ind);


%     figure(a);
%     plot(data(ind,11),(data(ind,9)*-1));
% %     title(['a'])
% %     title(['' num2str(data(a,5)) num2str(data(a,6)) num2str(data(a,13))
''])
% %     title(['' num2str(s(a,1))'']) %%% probably is not correct
% %     title (s(a,1:3)) %%% correct name but i cannot find solution ACC
% %   title([raw{find(ind,1),3},'-',num2str(raw{find(ind,1),14})])
%     ylabel('depth(cm)')
%     xlabel('dO18')

 end
 %%

     NCFile='12.nc';

    ncdisp(NCFile);
  loc_cor=cat,(2,cat(1,CORE_struct.Lat),cat(1,CORE_struct.Lon));

  lon=ncread(NCFile,'longitude');
  lat=ncread(NCFile,'latitude');
```

```
  tim=ncread(NCFile,'time');

  sd=ncread(NCFile,'sd');
  tp=ncread(NCFile,'tp');
  rsn=ncread(NCFile,'rsn');
%%

  loc_cor_pos(:,1)=interp1(lat,1:length(lat),loc_cor(:,1),'nearest');
  loc_cor_pos(:,2)=interp1(lon,1:length(lon),loc_cor(:,2),'nearest');


    tim = single (tim);
    sd  = single(sd);
    rsn = single(rsn);
    tp  = single(tp);
    sd_m = (sd./rsn*1e3);

   %%

    date=tim./24;
    date=date+datenum([1900,01,01,0,0,0]);


    Date_matrix= datevec([double(date)]);
    Date_letter= datestr([double(date)]);

    date_m=[date,Date_matrix];


%%
    NAO= xlsread('nao.xlsx');

    NAO=NAO(21794:end,:);
    NAO=[(datenum(NAO(:,1),NAO(:,2),NAO(:,3))),NAO];


    ind_date=date_m(:,4)==1;
    ind_month=date_m(:,3)==9;
    first_sep_year=ind_date & ind_month;

    starting_date=date_m(first_sep_year,:);

starting_date_pos=intearp1(date,1:length(date),starting_date(:,1),'nearest')
;
    starting_date=[starting_date_pos,starting_date];

    sampling_date=cellfun(@datenum,cat(1,CORE_struct.Date));
    sampling_date_pos=interp1(date,1:length(date),sampling_date,'nearest');
    sampling_date=[sampling_date_pos,sampling_date,[CORE_struct.Year]'];

%%
    for i=1:length(sampling_date);

            if sampling_date(i,3)==2015;
                start_core_pos(i)=starting_date(6,1);

                elseif sampling_date(i,3)==2014;
```

```
                start_core_pos(i)=starting_date(5,1);

                elseif sampling_date(i,3)==2013;
                start_core_pos(i)=starting_date(4,1);

                elseif sampling_date(i,3)==2012;
                start_core_pos(i)=starting_date(3,1);

                elseif sampling_date(i,3)==2011;
                start_core_pos(i)=starting_date(2,1) ;

                else sampling_date(i,3)==2010;
                start_core_pos(i)=starting_date(1,1);

        end
    end

 sam_star_d =[sampling_date,start_core_pos'];
%%

 for i=1:length(loc_cor_pos);

c=sd(loc_cor_pos(i,2),loc_cor_pos(i,1),((sam_star_d(i,4)):(sam_star_d(i,1)))
);
    z1 = squeeze(c);

     a=((sam_star_d(i,4)):(sam_star_d(i,1)));

     ind_first_snow=find(z1>0,1,'first');
     first_snow_dpos_day(i)=ind_first_snow;
     first_snow_pos_day=first_snow_pos_day';

     ind_last_without_snow=find(z1==0,1,'last');
     last_without_snow_pos_day(i)=ind_last_without_snow;
     last_without_snow_pos_day=last_without_snow_pos_day';

     ww(i)=w(last_without_snow_pos_day(i));
     ww=ww' ;
 end

%%

  sam_star_d =[sampling_date,start_core_pos',ww'];


for i=1:length(loc_cor_pos);

c=sd_(loc_cor_pos(i,2),loc_cor_pos(i,1),((sam_star_d(i,5)):(sam_star_d(i,1))
));


c=tp(loc_cor_pos(i,2),loc_cor_pos(i,1),((sam_star_d(i,5)):(sam_star_d(i,1)))
);
    z2 = squeeze(c);
```

```
c=NAO_prec(loc_cor_pos(i,2),loc_cor_pos(i,1),((sam_star_d(i,5)):(sam_star_d(
i,1))));
    z3 = squeeze(c);

    z3=NAO((sam_star_d(i,5)):(sam_star_d(i,1)),5);



CORE_struct(i).Samp_Date_number=sam_star_d(i,2);
CORE_struct(i).Samp_Date_Pos=sam_star_d(i,1);
CORE_struct(i).First_Snow_Pos=sam_star_d(i,5);

CORE_struct(i).sd=z1;
CORE_struct(i).tp=z2;
CORE_struct(i).NAO=z3;
end

%%
for i=1:length(loc_cor_pos);
    a(i)=max((CORE_struct(i).Depth));
    b(i)= CORE_struct(i).sd(end);
end

coefficient_rescale=(b./a)';

  for i=1:length(loc_cor_pos);

      x_res=CORE_struct(i).Depth;
      x_res=a(i)-x_res;

      CORE_struct(i).Rescale_obs_depth=x_res*coefficient_rescale(i);

  end

%%

for j=1:size(loc_cor_pos,1);


        x_res=CORE_struct(j).Rescale_obs_depth;
        x_sd=CORE_struct(j).sd;
        x_up=cat(1,false(1),diff(x_sd)>0);

        time=NaN(size(x_res),'single');
        gap=false(size(x_res));

   for i=1:length(x_res);

     tmp = (x_sd<=x_res(i)) & x_up;
     if any(tmp)
        time(i)=find(tmp,1,'last');
     else
         time(i)=1;
     end

   end
```

```
   CORE_struct(j).Time=time;

   x_nao=CORE_struct(j).NAO;

   CORE_struct(j).NAOtime=x_nao(CORE_struct(j).Time)

   [CORE_struct(j).co_ef,CORE_struct(j).co_p]=
corrcoef(CORE_struct(j).NAOtime,CORE_struct(j).d18O);

   CORE_struct(j).co_ef_n=CORE_struct(j).co_ef(1,2);
   CORE_struct(j).co_p_n=1-CORE_struct(j).co_p(1,2);

   CORE_struct(j).d_excess = CORE_struct(j).dD- 8*CORE_struct(j).d18O;

   CORE_struct(j).co_ef_dexcess =
corrcoef(CORE_struct(j).NAOtime,CORE_struct(j).d_excess);
   CORE_struct(j).co_ef_dexcess_n=min(min(CORE_struct(j).co_ef_dexcess));

   CORE_struct(j).date= double(CORE_struct(j).Samp_Date_number-
length(x_sd)+time)
   CORE_struct(j).date_letter= datestr([double(CORE_struct(j).date)]);


   clf

   subplot(1,2,1)
   hold on
   plot(double(CORE_struct(j).Samp_Date_number-[length(x_sd)-1:-1:0]),...
        x_sd,'b*-')
    plot(double(CORE_struct(j).Samp_Date_number-length(x_sd)+time),...
        x_res,'ro','MarkerSize',10)
    title(sprintf('%s-%04i',CORE_struct(j).Site{1},CORE_struct(j).Year))
    datetick('x','mmm.yy')
    ylabel('Depth')

 subplot(1,2,2)
    plot(CORE_struct(j).d18O,...
        double(CORE_struct(j).Samp_Date_number-length(x_sd)+time),...
        'ro-','LineWidth',2)
    title(sprintf('%s-%04i',CORE_struct(j).Site{1},CORE_struct(j).Year))
    datetick('y','mmm.yy')
    xlabel('d18O')

     subplot(1,2,1)
   hold on
   plot(double(CORE_struct(j).Samp_Date_number-[length(x_nao)-1:-1:0]),...
        x_nao,'k.-')
    plot(double(CORE_struct(j).Samp_Date_number-length(x_nao)+time),...
        x_res,'ro','MarkerSize',10)
    title(sprintf('%s-%04i',CORE_struct(j).Site{1},CORE_struct(j).Year))
    datetick('x','mmm.yy')
    ylabel('Depth')

   subplot(1,2,1)
   hold on
   plot(double(CORE_struct(j).Samp_Date_number-[length(x_sd)-1:-1:0]),...
        x_sd,'b*-')
```

```
    plot(double(CORE_struct(j).Samp_Date_number-length(x_sd)+time),...
        x_res,'ro','MarkerSize',10)
    title(sprintf('%s-%04i',CORE_struct(j).Site{1},CORE_struct(j).Year))
    datetick('x','mmm.yy')
    ylabel('Depth')


     subplot(1,3,2)
    plot(CORE_struct(j).d18O,...
        double(CORE_struct(j).Samp_Date_number-length(x_sd)+time),...
        'ro-','LineWidth',2)
    title(sprintf('%s-%04i',CORE_struct(j).Site{1},CORE_struct(j).Year))
    datetick('y','mmm.yy')
    xlabel('d18O')

     subplot(1,2,2)
     hold on
     x1=CORE_struct(j).d18O;
     y1=(double(CORE_struct(j).Samp_Date_number-length(x_sd)+time));
     x2=CORE_struct(j).NAO;
     y2=double(CORE_struct(j).Samp_Date_number-[length(x_nao)-1:-1:0]);
     x3=CORE_struct(j).NAO*(-1);
     y3=double(CORE_struct(j).Samp_Date_number-[length(x_nao)-1:-1:0]);

line(x1,y1,'Color','r','LineWidth',1.5,'marker','s')
ax1 = gca;
ax1.XColor = 'r';
ax1.YColor = 'r';
datetick('y','mmm.yy')
    xlabel('d18O')
set(ax1,'ylim',[(y2(1)) (y2(end))])

ax1_pos = ax1.Position;
ax2 = axes('Position',ax1_pos,...
    'XAxisLocation','top',...
    'YAxisLocation','right',...
    'Color','none');


line(x2,y2,'Parent',ax2,'Color','k','lineStyle',':','LineWidth',1)
    title(sprintf('%s-%04i',CORE_struct(j).Site{1},CORE_struct(j).Year))
    title(sprintf('%s-%04i   (%s
%.2f)',CORE_struct(j).Site{1},CORE_struct(j).Year,'R=',CORE_struct(j).co_ef_
n))
    datetick('y','mmm.yy')
   xlabel(['NAO','-','R',num2str(CORE_struct(j).co_ef_n)])
    xlabel('NAO')
set(ax2,'ylim',[(y2(1)) (y2(end))])


line(x3,y3,'Parent',ax2,'Color','m','lineStyle',':','LineWidth',1)
    title(sprintf('%s-%04i',CORE_struct(j).Site{1},CORE_struct(j).Year))
    datetick('y','mmm.yy')
    xlabel('NAO')


 subplot(1,3,3)
```

```
        plot(CORE_struct(j).NAO,...
        double(CORE_struct(j).Samp_Date_number-[length(x_nao)-1:-1:0]),...
        'k.-','LineWidth',2)
    title(sprintf('%s-%04i',CORE_struct(j).Site{1},CORE_struct(j).Year))
    datetick('y','mmm.yy')
    xlabel('NAO')



w=[734008:1:734259];
x=CORE_struct(j).d18O;
y=double(CORE_struct(j).Samp_Date_number-length(x_sd)+time);
plot(x,y,'k.-','LineWidth',1.5)
plot(CORE_struct(j).d18O,...
         double(CORE_struct(j).Samp_Date_number-length(x_sd)+time),...
         'k.-','LineWidth',1.5)

ylim ([734035 734245]);

set(ax2,'ylim',[(y2(1)) (y2(end))])
set(y,'ylim',[(w(1)) (w(end))])
title(sprintf('%s-%04i',CORE_struct(j).Site{1},CORE_struct(j).Year))
    datetick('y','mmm.yy')
    xlabel('d18O')


az = 90;
el = 90;
view(az, el)

     x1=CORE_struct(j).d18O;
     y1=(double(CORE_struct(j).Samp_Date_number-length(x_sd)+time));
     x2=CORE_struct(j).NAO;
     y2=double(CORE_struct(j).Samp_Date_number-[length(x_nao)-1:-1:0]);
     x3=CORE_struct(j).NAO*(-1);
     y3=double(CORE_struct(j).Samp_Date_number-[length(x_nao)-1:-1:0]);

line(x1,y1,'Color','k','LineWidth',1.5,'marker','s')
ax1 = gca;
ax1.XColor = 'k';
ax1.YColor = 'k';
datetick('y','mmm.yy')
    xlabel('d18O')
set(x1,'ylim',[(y2(1)) (y2(end))])

ax1_pos = ax1.Position;
ax2 = axes('Position',ax1_pos,...
    'XAxisLocation','top',...
    'YAxisLocation','right',...
    'Color','none');

    plot_name=sprintf('png/Profile.%s-%04i.png',...
        CORE_struct(j).Site{1},CORE_struct(j).Year);
     plot_name=sprintf('png/Profile.%04i-%s.png',...
        CORE_struct(j).Year,CORE_struct(j).Site{1});

title(sprintf('%s-%04i',CORE_struct(j).Site{1},CORE_struct(j).Year))
```

```
      datetick('y','mmm.yy')

      plot_name=sprintf('png/Profile.%04i-%s.png',...
         CORE_struct(j).Year,CORE_struct(j).Site{1});

     if ~exist('png','dir')
         mkdir('png')
     end
     print(plot_name,'-dpng','-r300');
     pause(10)

end
```

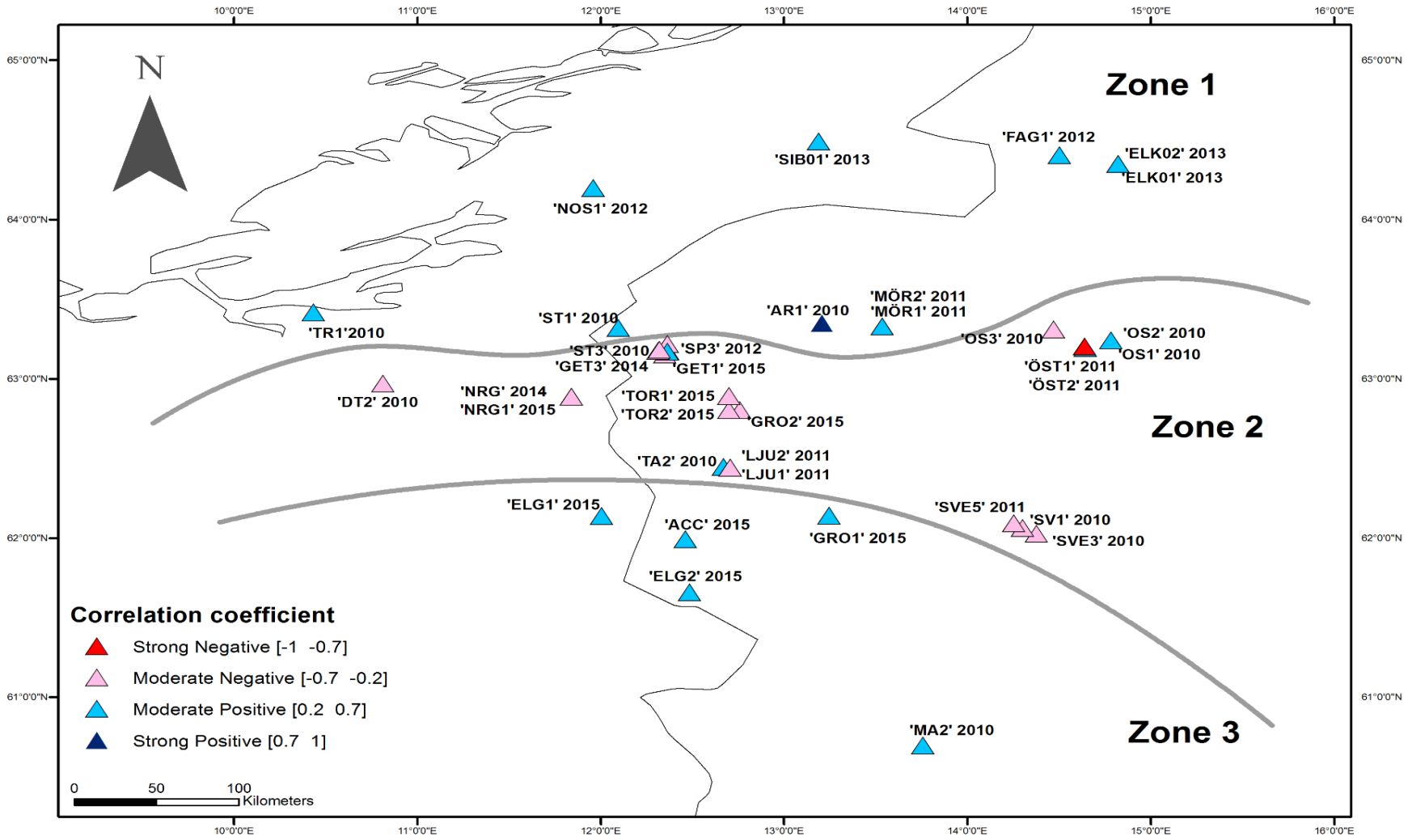

Figure 1: Central Scandinavia (Jämtland). Detailed map of the study region.